In Vitro Release of Curcumin from

Polymeric Nanoparticles Using Two-Phase System

BY

CATALINA MOGOLLON
B.S., University of Illinois at Chicago, Chicago, 2009

THESIS

Submitted as partial fulfillment of the requirements
for the degree of Master of Science in Chemical Engineering
in the Graduate College of the
University of Illinois at Chicago, 2016

Chicago, Illinois

Defense Committee:

Ying Liu, Chair and Advisor, Chemical Engineering
Lewis E. Wedgewood, Chemical Engineering
Brian P. Chaplin, Chemical Engineering

This thesis is dedicated to my husband, Nibras Obaid, and my son, Ishmael Obaid, without whom it would never have been accomplished.

ACKNOWLEDGMENTS

I would first like to thank Dr. Ying Liu who accepted me as a member of her group and provided me with an interesting research project. I also want to thank Dr. Liu for all her support to complete this thesis. I would like to give my special thanks to a member of the group, Magdalena Szymusiak, who continuously supported me with her advice, work, and experience during my research project. Magdalena initially showed me the set-up of the release system. She later trained me in the use of HPLC, and most importantly she prepared the nanoparticles encapsulating the model compound employed in this study. Another member of the group who I would like to thank is Pin Zhang who performed useful Langmuir-trough experiments of phospholipids. I would also like to acknowledge Dr. Brian Chaplin who allowed me to have access to his laboratory and equipment in order to complete my experiments. Finally, the completion of this research project and thesis would not have been possible without my family support. Thus, I want to say thank you to all.

CM

TABLE OF CONTENTS

LIST OF TABLES

LIST OF FIGURES

LIST OF FIGURES (continued)

ABSTRACT

In vitro models to measure the release of hydrophobic compounds from polymeric nanocarriers are investigated and compared. The release models consist of a two-phase system. An aqueous solution in the bottom layer contains suspended polymeric nanoparticles encapsulating a hydrophobic compound. A water-immiscible organic solvent of lower density is used to extract the compound from the aqueous phase. This system overcomes the solubility limitation of hydrophobic compounds in aqueous solutions. It provides a faster and more convenient way to characterize the *in vitro* release of hydrophobic compounds from nanoparticles. Poly(lactic-co-glycolic acid) (PLGA) nanoparticles with negative surface charges and poly(ethylene glycol) methyl ether-block-poly(lactide-co-glycolide) (PEG-PLGA) nanoparticles with neutral surface brushes encapsulating curcumin were used in this study. Three types of interfaces were tested: (1) liquid-liquid interface, (2) phospholipid packed interface, and (3) dialysis membrane interface. In the first case, relatively quicker release of curcumin from both types of polymeric nanoparticles was recorded, which was mainly caused by the direct contact of particles with the organic solvent at the liquid-liquid interface. The release was independent of solution pH. In the second case, monolayers of amphiphilic molecules with different packing strength (such as phospholipids with and without cholesterol and PEGylated phospholipids) were formed at the liquid-liquid interface to depict biological barriers. The self-assembled monolayers at the interface did not provide a sufficient energy barrier to decrease the collision rate of the particles occurring at the liquid-liquid interface, and the release rate of curcumin was similar as the one measured using the first system. The third *in vitro* release model with a dialysis membrane at the interface using a custom-designed glass cell completely prevented the contact of particles with the organic solvent, resulting in a diffusion-controlled

drug release profile of curcumin. The mathematical 1D diffusion analysis was applied to reveal the sensitivity of diffusivity of the compound in the organic solvent and partition coefficient of the compound in each phase of the solutions.

1 INTRODUCTION

1.1 Background

1.1.1 Polymeric Nanoparticles Encapsulating Hydrophobic Drugs

Polymeric nanoparticles encapsulating drug compounds are generally less than 1 um in diameter with a matrix type structure made of a synthetic or natural polymer in which drugs can be entrapped inside the particle.[1, 2] Two types of polymeric nanoparticles are presented here in this study: (1) poly(lactic-co-glycolic acid) (PLGA) nanoparticles with negatively charged surface and (2) poly(ethylene glycol) methyl ether-block-poly(lactide-co-glycolide) (PEG-PLGA) nanoparticles with neutral PEG brushes on the surface. PLGA and PEG polymers are used for the formulation of nanoparticles due to their biocompatibility and biodegradability attributes.[2] The encapsulation of drugs into polymeric nanoparticles has been developed by Liu group for oral delivery of several hydrophobic compounds to improve target drug delivery and decrease unwanted side effects.[3, 4] The well-controlled size distribution of these particles has been found to be important for improving cellular uptake and bioavailability of drug compounds.[1, 4, 5] Polymeric nanoparticles with their highly hydrophilic surface have also been designed to improve particles blood circulation time, solubility, and stability. The hydrophobic core of polymeric nanoparticles increases the encapsulation of compounds through hydrophobic interaction.[6, 7]

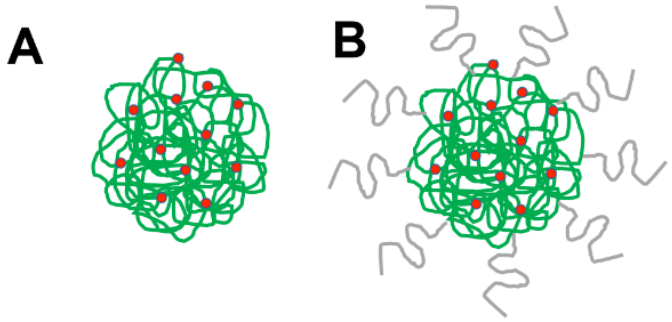

Figure 1. Two types of polymeric nanoparticles: **(A)** PLGA curcumin nanoparticles and **(B)** PEG-PLGA curcumin nanoparticles.

For the present study, curcumin, a hydrophobic compound with low molecular weight has been used as the model compound to be encapsulated into the polymeric nanoparticles. Curcumin is a natural polyphenol that is extracted from Turmeric, the herbal remedy Curcuma Longa.[8] The molecular structure of curcumin, diferuloylmethane [1,7-bis(4-hydroxy-3-methoxyphenyl)-1,6-heptadiene-3,5-dione] is presented in **Figure 2**. Curcumin has many valuable pharmaceutical advantages such as anti-inflammatory, anti-cancer, anti-oxidant, anti-amyloid, anti-depressant, and anti-tumor.[9-12] The recent research in Liu group also discovered that curcumin could attenuate or even reverse morphine tolerance and dependence.[4, 13] However, curcumin has low solubility in water, poor bioavailability, rapid metabolism, and low stability at neutral pH.[9] Moreover, it generally degrades fast at neutral pH conditions.[9] The polymeric nanoparticles protect curcumin from fast degradation and increase its bioavailability.

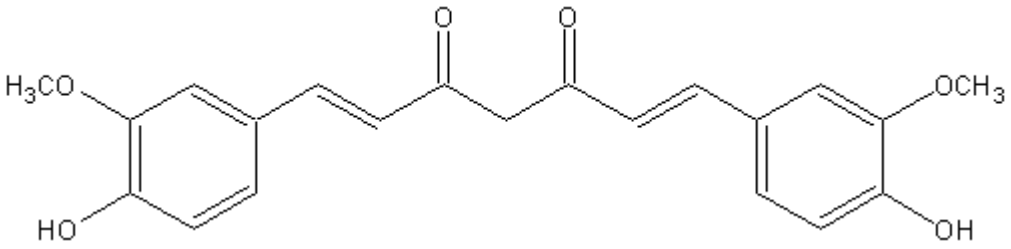

Figure 2. Molecular structure of curcumin.

1.1.2 Flash nanoprecipitation process used to generate nanoparticles

Polymeric nanoparticles have been prepared by different methods, among which the most important ones are emulsification, sonication, critical processing, and nanoprecipitation methods.[2, 10] However, the previous methods have major disadvantages such as broad size distribution and low drug loading.[10] On the other hand, flash nanoprecipitation (FNP) is a kinetic control process for the formulation of polymeric nanoparticles encapsulating hydrophobic drugs with relatively high drug loading. Rapid micro-mixing of a solution of polymer and drug dissolved in a water-miscible solvent with the aqueous anti-solvent solution causes nanoparticle precipitation in milliseconds.[11] This process achieves controllable nanoparticle sizes by matching the kinetics of polymer micellization and drug nucleation and growth.[10-12] Mixers with different geometries, such as an impinging jet and a multi-inlet vortex mixer (MIVM) have been used for the preparation of polymeric nanoparticles by flash nanoprecipitation.[10] In this study, the MIVM (**Figure 3**) is used for the preparation of nanoparticles by flash nanoprecipitation for the additional advantages of flexible inlet-stream arrangements of the MIVM.[10]

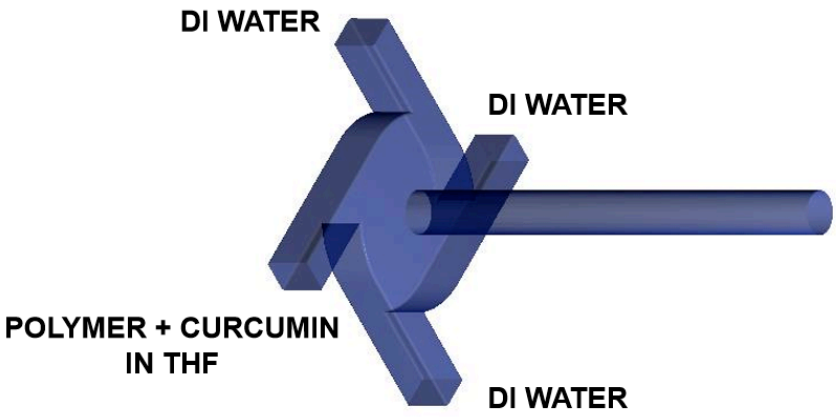

Figure 3. Schematic of MIVM.

1.1.3 Current *in vitro* release models

In general, after the oral administration of polymeric nanoparticles, the *in vivo* release of drugs to the blood circulation happens through three different mechanisms. (1) The drug is released from the polymeric nanoparticles early before they even reach the blood circulation. In this case, the nanoparticle stability has to be addressed upon environmental changes (such as pH and temperature) to protect the drug from early release and metabolism. (2) The polymeric nanoparticles are attached to a mucus layer of the human intestinal epithelium, and the free drug is then released and later reaches the blood circulation system.[14] (3) The polymeric nanoparticles cross biological barriers to reach the blood circulation. Lymphoid uptake is mainly responsible for the last mechanism in which the uptake of polymeric nanoparticles takes place through highly specialized enterocytes, absorptive cells referred as M cells, which constitute the follicle-associated epithelium, a part of the intestinal tissue, named as the Peyer's patches. [14-16] Understanding the *in vivo* mechanisms of the release of drugs from polymeric nanoparticles is essential in order to optimize the design of the nanoparticles. However, *in vivo* models are very

expensive and less reproducible. Therefore, it is necessary to develop *in vitro* release models for comparing material properties and predicting the compound behavior *in vivo*.

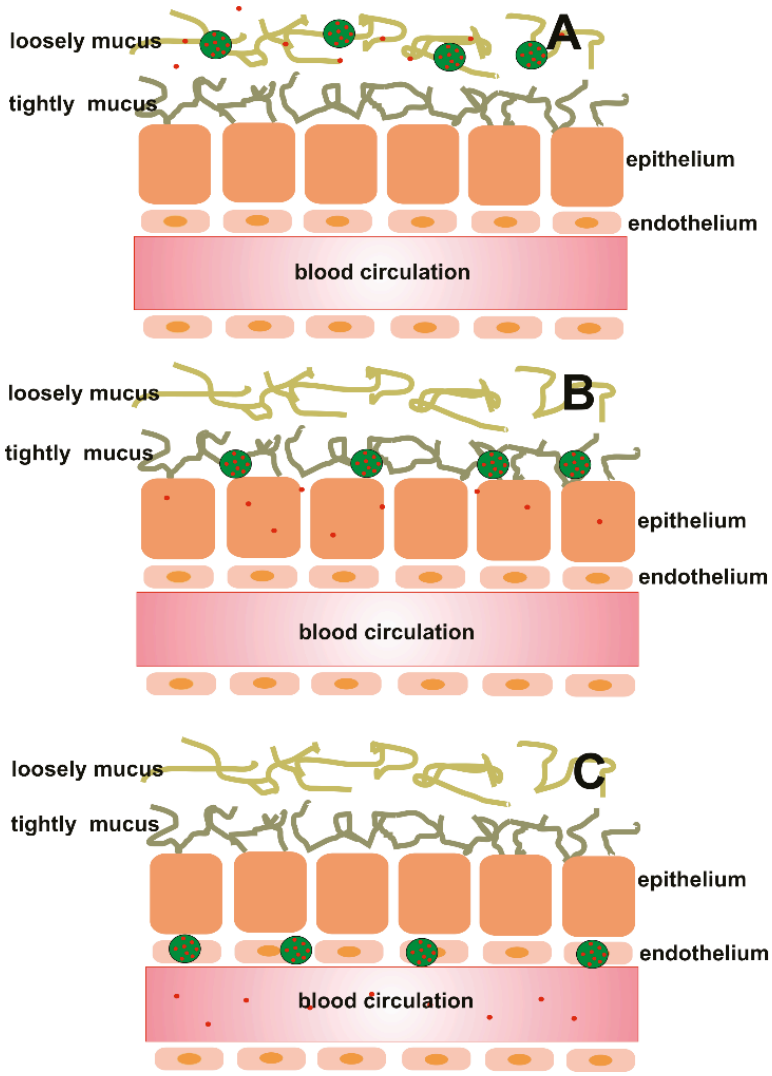

Figure 4. Possible *in vivo* mechanisms of the release of drugs from polymeric nanoparticles. **(A)** Drug is released in the loosely mucus. **(B)** Polymeric nanoparticles are attached to the epithelium by the firmly mucus. **(C)** Polymeric nanoparticles cross the biological barriers and reach the blood circulation.

Existing methods for testing *in vitro* release of compounds from polymeric nanoparticles have been limited to the dialysis diffusion method[17] and the dissolution method.[8] However, these methods require tedious setup and may cause misleading results. The main limitation of the dialysis method is the low solubility of the hydrophobic compound in aqueous buffers. The dissolution method may cause early release of the compound from the nanoparticles during centrifugation. Moreover, addition of surfactants into the release medium may be necessary for the dissolution method to minimize the stirring effects which could affect the quantification of the compound during HPLC analysis. Additional purification or exaction processes may also be required for the dissolution method.

1.2 Project Goals

The goal of this research is to develop an *in vitro* release model using a two-phase system to study the release of hydrophobic compounds from polymeric nanoparticles, decoupling the diffusion and dissolution processes. The aqueous phase contains the nanoparticles suspended in buffer solutions of a specific pH value. The organic solvent phase is used to extract the hydrophobic compound from its saturated aqueous phase. This method solves the problem of limited drug solubility in aqueous solutions while maintain sink conditions. This *in vitro* release method is simple and inexpensive. **Figure 5** and **Figure 6** show the initial set up of the two-phase *in vitro* release system designed for this study. Various types of molecules (such as phospholipids and membrane proteins) and layers (such as dialysis membrane) have been used to separate the two phases to mimic biological systems and to decouple the effects of diffusion from dissolution.

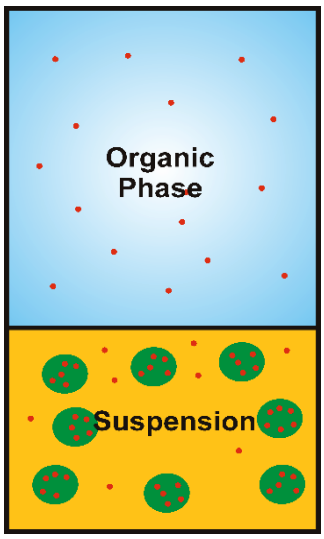

Figure 5. Schematic of the two-phase *in vitro* release system.

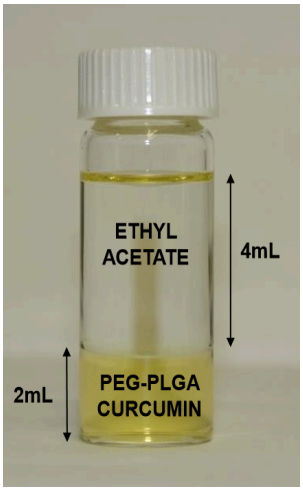

Figure 6. *In vitro* release of curcumin from PEG-PLGA curcumin nanoparticles at pH 7.4 using a two-phase system.

Phospholipids, the principal component of cell membranes, in living organisms consist of two distinct parts. Tails of phospholipids are hydrophobic whereas heads are hydrophilic.[18] **Figure 7** shows 1,2-distearoyl-sn-glycero-3-phosphocholine (DSPC) one of the phospholipids

used in this study. Thus, phospholipids can self-assemble on the organic-water interface with the heads in the aqueous phase and the tails pointing out into the organic phase.

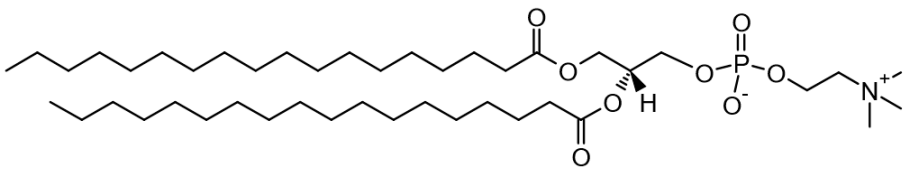

Figure 7. Molecular structure of DSPC.

By introducing phospholipids at the liquid-liquid interface, the *in vitro* release model represents biological barriers at a certain level (**Figure 8**).

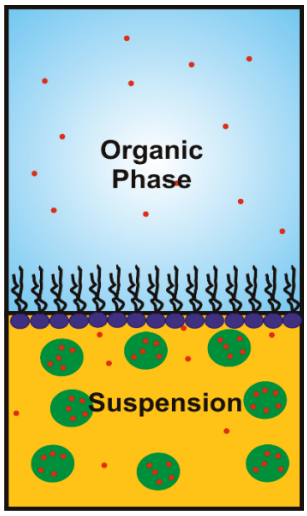

Figure 8. Two-phase *in vitro* release system with phospholipids.

To increase the energy barrier, phospholipids with cholesterol or with PEGylated phospholipids at the liquid-liquid interface of the release model were tested. In the case of phospholipid-cholesterol mixture, strong attractions between cholesterol and phospholipid molecules occurs by a condensing effect. When the mixture is arranged into a monolayer, the

condensing effect results in higher order of hydrocarbon chains of phospholipids, lower gauche defects in phospholipid tails, and higher packing density.[19-21] The strongest attractions for this mixture occur around 30-35% molar concentration of cholesterol.[21, 22] In addition, mixture of phospholipids with PEGylated phospholipids were used to further increase the energy barrier. PEGylated phospholipids are commonly used for the formation of liposomes, which prolong the circulation life time, and improve pharmacokinetics and therapeutic efficacy of encapsulated drugs in liposomes.[22] The addition of PEG to phospholipids generates steric repulsive forces which prevent the fusion and disruption of the liposomes.[23] According to the report of Chou et al., the strongest steric repulsive interactions occurs at 5mol% DPSE-PEG_{2k}.[23] **Figure 9** shows the schematic of the *in vitro* release system using phospholipids, cholesterol, and PEGylated phospholipids at the liquid-liquid interface.

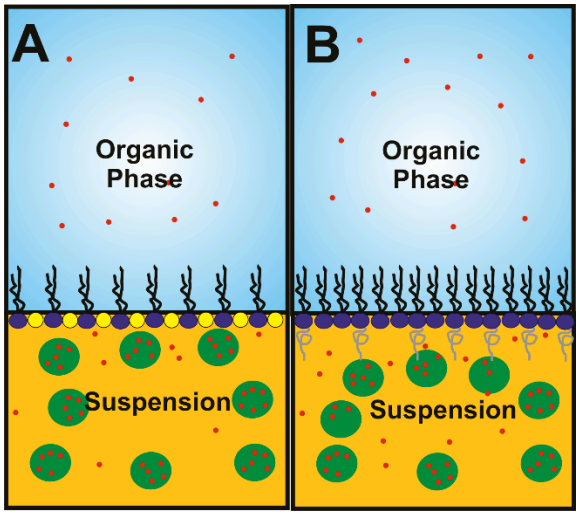

Figure 9. Two-phase release system with **(A)** phospholipids and cholesterol and **(B)** phospholipids and PEGylated phospholipids at the liquid-liquid interface.

A dialysis membrane layer was also added to the interface to completely prevent particles from contacting the organic phase. Therefore, in this model, the release is completely diffusion-controlled. Dialysis membranes are semi-permeable layers that separate molecules based on the membrane pore size indicated by a molecular weight-cutoff (MWCO). A membrane's MWCO is the smallest average molecular mass in Daltons (Da) of a molecule that will not diffuse through the membrane. Dialysis membranes are compatible with a wide range of pH, temperature, and mainly organic solvents. **Figure 10** and **Figure 11** show the experimental set up of the *in vitro* release using a two-phase system and a dialysis membrane layer.

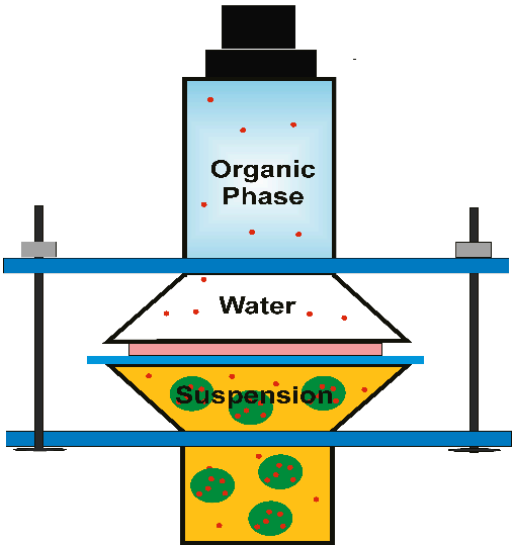

Figure 10. Schematic of *in vitro* release in glass cell with dialysis membrane.

Figure 11. Experimental set up of in vitro release in glass cell with dialysis membrane.

In this study, a custom-made glass cell is used to incorporate the dialysis membrane at the organic-water interface of the release system. The glass cell was constructed with two standard 15mm ID O-ring joints and an extra 15 mm ID tube with polypropylene screw cap. The length of the two joints was modified to represent the liquid volumes of the two phases in the release model. The lower compartment of the cell is 13mm long and has 2mL capacity. The upper compartment is 50mm long and has about 8mL in capacity. Besides, the extra tube with incorporated screw cap was fused to the top of the upper compartment to create an easy sampling port and to avoid evaporation of the solvent. The final design of the glass cell with a Teflon O-ring and clamps is presented in **Figure 12** and **Figure 13**.

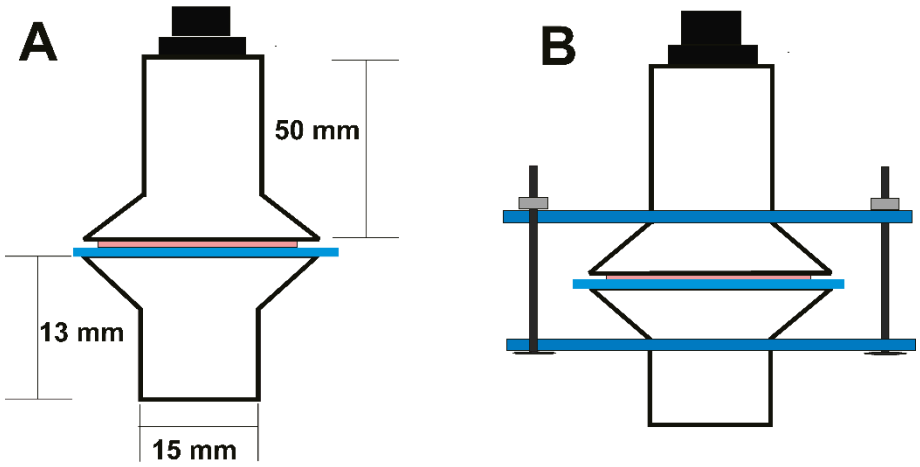

Figure 12. Final design of customized glass cell with dialysis membrane for the *in vitro* release. **(A)** Dimensions of glass cell. **(B)** Glass cell with horse pinch clamp.

Figure 13. Picture of final diffusion cell used during experiments.

2 EXPERIMENTAL SECTION

2.1 Materials and Reagents

Curcumin (77% purity), potassium phosphate monobasic (99.0%), dimethylsulfoxide (DMSO), acetonitrile (HPLC grade), formic acid (Aldehyde Free Sequencing Grade), ethyl acetate (LC_MS CHROMASOL V), PLGA (acid terminated; PLA/PGA 50:50 w:w, M_w = 7000-17000), PEG-PLGA (M_w = 2000-4500), tetrahydrofuran (THF), leucine, and trehalose where all purchased from Sigma-Aldrich (St. Louis, MO). Thermo Scientific Hypersil gold C18 column (2.1 × 50nm, 5μm) was acquired from Fischer Scientific (Pittsburg, PA). Phospholipids: Egg PC (L-α-phosphatidylcholines), DPPC (1,2-dipalmitoyl-sn-glycero-3-phosphocholine), DSPC (1,2-distearoyl-sn-glycero-3-phosphocholine), and DPPE-PEG_{2k} (N-(carbonyl-methoxypolyethyleneglycol2000)-1,2-dipalmitoyl-sn-glycero-3-phosphoethanolamine) were purchase from Avanti Polar Lipids (Alabaster, AL). Cholesterol was kindly provided by, Dr. Perez-Salas, Assistant Professor from the Department of Physics at UIC. SpectraPor dialysis membrane (MWCO: 6-8,000 Da) was acquired from Spectrum Labs, Inc. (Rancho Dominguez, CA).

2.2 General Methods

2.2.1 Preparation of Phosphate Buffer Solutions

Buffer solutions were prepared at 10mM of potassium phosphate monobasic. Millipore water with conductivity of 18.2 M-Ω×cm was used for all aqueous solutions. The pH value of the buffer solutions was adjusted to pH 2, pH 5, and pH 7.4 using 5% (w/v) NaOH and 5% (v/v) HCl.

2.2.2 Extraction of Curcumin from Polymeric Nanoparticles

The extraction of curcumin was performed with 400 µL curcumin nanoparticles suspension and 800 µL organic solvent (ethyl acetate) in micro-centrifugation tubes. The samples were vortexed for 5 minutes and then centrifuged for 10 minutes at 350rpm.

2.2.3 Quantification of Curcumin by HPLC

The amount of accumulative release of curcumin to the organic phase was quantified using a high performance liquid chromatographic (HPLC) with a PDA detector and autosampler. A Hypersil gold C18 column (2.1 × 50nm, 5µm) column was used. Liquid chromatography (LC) conditions consisted of a gradient method. The mobile phase run from 5% to 95% acetonitrile with formic acid solution (0.1% v/v) during 8 minutes, followed by 4 minutes of equilibrium. The flow rate was set to be 0.3mL/min. Samples injection volume was 10 µL. The concentration of curcumin was determined using a standard curve of curcumin in ethyl acetate. The typical figure to show the separated peak of curcumin using HPLC is shown in **Figure 14**.

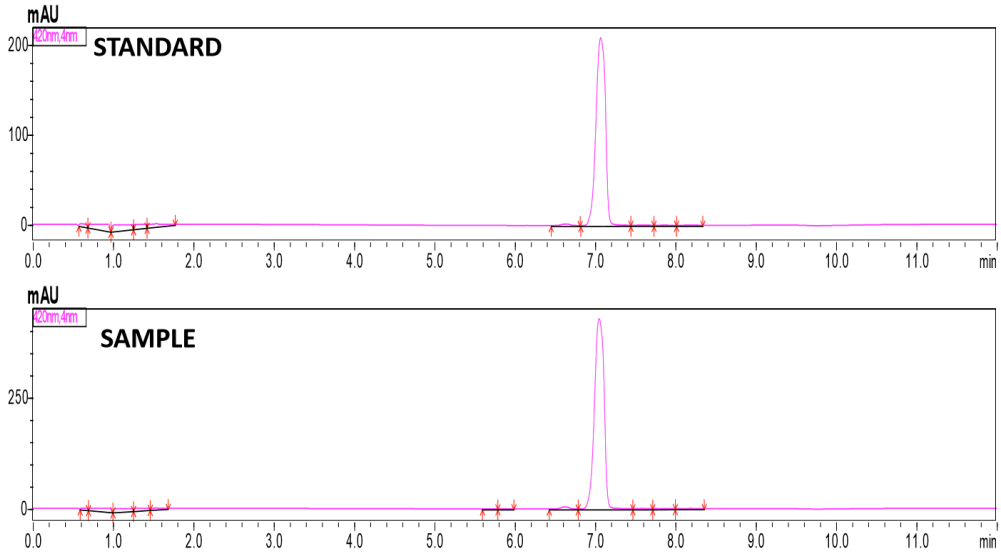

Figure 14. HPLC chromatogram of curcumin peak at wavelength 420 nm.

2.2.4 Degradation Control of Curcumin from Polymeric Nanoparticles

PEG-PLGA curcumin nanoparticles were resuspended at 20 mg/mL of total solid concentration (11 μg/mL curcumin concentration) in phosphate buffer solutions at pH 7.4, pH 5, and pH 2 followed by sonication for 25 minutes using a bath sonicator (Branson, CPXH Ultrasonic Bath, Emerson Industrial Automation). The controls were performed in triplicates for all three pH values. Samples were incubated at 37°C. At different time points (0hr, 24hr, 48hr, 72hr, and 96hr) 400 μL aliquots of samples were collected and curcumin was extracted as described in section 2.2.2.

2.2.5 Nanoparticles Formation and Characterization

The model compound, curcumin, was encapsulated in PLGA and PEG-PLGA polymers at polymer to drug ratios of 1:1 and 5:1 by mass respectively using the MIVM. The PLGA curcumin nanoparticles at 1:1 polymer to drug ratio were prepared with 0.2wt% PLGA and 0.2wt% curcumin dissolved in THF mixed with Millipore water. The PEG-PLGA curcumin nanoformulation at 5:1 polymer to drug ratio was prepared with 0.2wt% PEG-PLGA and 0.04wt% curcumin dissolved in THF mixed with Millipore water. Nanoparticles in solution were immediately frozen at -80°C and then freeze dried for 2-3 days using a freeze dryer (Labconco, FreezeZone 1 Liter Console, Freeze Dry Systems, Kansas City, MO) at -47°C and vacuum pressure. Trehalose (300:1 weight ratio to the nanoparticles) and leucine (5:1 weight ratio to the nanoparticles) were used as excipients to prevent permanent particle fusion and aggregation during freeze drying.

Dried polymeric nanoparticles were resuspended in 10mM phosphate buffer solution at pH 7.4, pH 5, and pH 2. PLGA nanoparticles suspensions were prepared at 10 mg/mL total solid

concentration (16 μg/mL curcumin concentration) and sonicated for 5 minutes. PEG-PLGA nanoparticles were resuspended at 20 mg/mL for total solid (11 μg/mL curcumin concentration) and sonicated for 25 minutes.

Nanoparticles size distribution after resuspension was measured by Dynamic Light Scattering (DLS) (Malvern, Zetasizer Nano ZS90, Worcestershire, U.K.). The size of THE nanoparticles was presented as intensity-weighted diameter.

The encapsulation efficiency (EE) of PLGA curcumin and PEG-PLGA curcumin nanoparticles was determined by dissolving the nanoparticles in DSMO. PLGA curcumin and PEG-PLGA curcumin nanoparticles were dissolved at 3 mg/mL of total solid (5 μg/mL curcumin concentration) and at 15 mg/mL of total solid (8 μg/mL curcumin concentration) respectively. UV-vis spectrophotometer (Shimadzu, UV-1601) was used to quantify the amount of encapsulated curcumin at the absorbance wavelength of 435 nm.

2.2.6 Two-phase System Setup and Release Measurements

The *in vitro* release of curcumin was performed in triplicates for all cases presented. Suspensions of PLGA curcumin nanoparticles at 10 mg/mL total solid (16 μg/mL curcumin concentration) and PEG-PLGA curcumin nanoparticles at 20 mg/mL of total solid (11 μg/mL curcumin concentration) were prepared in 10mM phosphate buffer. Suspensions of PLGA curcumin nanoparticles were sonicated for 5 minutes whereas suspensions of PEG-PLGA curcumin nanoparticles were sonicated for 25 minutes.

The *in vitro* release was performed in an O.D. × H (17mm × 60 mm) glass vial without extra energy barrier at the interface. Three different combination of aqueous and organic phase volumes were designed: (1) 1mL of aqueous nanoparticle suspension and 2mL of ethyl acetate; (2) 2mL of nanoparticle aqueous suspension and 4mL of ethyl acetate; and (3) 2mL of

nanoparticles aqueous suspension and 2mL of ethyl acetate. Samples were incubated at 37 ºC and protected from light exposure. At specific time points (0.5, 2, 4, 6, 24, 48, 72, 96, 120, 144, 168 and 192 hours), 500 µL of organic solvent was collected and replaced with 500 µL fresh solvent to maintain same volume.

The accumulative release of curcumin to the organic phase as percentage was calculated using formula (1). In formula (1), total curcumin represents the total amount of curcumin based on the final extraction rather than the initial value to compensate the curcumin degradation. In this way, the 100% release of curcumin does not represent the initial total amount of curcumin used, but the total amount of curcumin that can be extracted from the suspension. The amount of extracted curcumin was calculated by using a set of calibration curve of curcumin in ethyl acetate measured on the same tray together with the samples.

$$\text{Release } (\%) = \frac{\text{Released Curcumin}}{\text{Total Curcumin}} \times 100\% \qquad (1)$$

2.2.7 Formation of Phospholipid Monolayers at the Liquid-Liquid Interface

The formation of phospholipid monolayers at the liquid-liquid interface of two immiscible solutions was accomplished by the Langmuir-Blodgett technique.[24] The method was originally designed to assemble a monolayer of phospholipids at the air-water interface. For this study, the monolayer was first formed at the air-aqueous (nanoparticles suspension) interface. Using a glass tight syringe with reinforce plunger (Hamilton, Model 1801 N SYR, Cemented NDL, 26s ga, 2 in, point style 2, Reno, NV, USA), 10 µL of phospholipids dissolved in chloroform were placed drop-by-drop onto the aqueous sub-phase. The solvent was then allowed to evaporate at room temperature for about 10 minutes.

The number of phospholipid molecules needed to be placed at the liquid-liquid interface was calculated with equation (2) based on the packing area per phospholipid molecule at 37°C (**Table 1**) and the cross sectional area of a 15mm ID glass vial. The amount of phospholipid molecules was then translated in terms of mass by formulas (3) and (4).

$$\text{phsopholipids molecules} = \frac{\text{cross sectional area glass vial}}{\text{packing area per phospholipid molecule}} \quad (2)$$

$$\text{phospholipids moles} = \text{phospholipids molecules} \times \frac{1\,\text{mole}}{6.023 \times 10^{23}\,\text{molecules}} \quad (3)$$

$$\text{phospholips grams} = \text{phospholipids moles} \times \text{phospholipid MW} \quad (4)$$

Table 1. Packing area per phospholipid molecule at 37°C.

Lipid	**Packing Area/Phospholipid ($Å^2$/molecule)**
L-α-PC [25]	70
DPPC [26]	60
DPPC-30%cholesterol [18, 27]	50
DSPC [28]	65
DSPC-30%cholesterol [29]	45
DSPC-5%DSPE-PEG_{2k} [23]	55

2.2.8 *In Vitro* Release System Set-up with Dialysis Membrane Layer

The *in vitro* release was performed in a customized 15mm ID glass cell. PEG-PLGA curcumin nanoparticles suspension (2mL) in phosphate buffer solution at pH 7.4 was added to the lower compartment of the glass cell. A piece of dialysis membrane (MWCO: 6-8kDa) was placed on top of the lower compartment. An excess of 500 μL aqueous nanoparticle suspension was added on top of the original 2mL suspension to avoid the formation of bubbles after the dialysis membrane was placed on top of the lower chamber. Teflon O-ring (116, 18.72 mm ID × 2.62 mm W) was allocated on top of the membrane, covered by the upper glass compartment. A pinch horse clamp was used to hold the two compartments tightly. Consecutively, 1mL of Millipore water was added into the top compartment to avoid solvent evaporation. Finally, 4mL of ethyl acetate were added slowly above the aqueous solution. The glass cell was sealed with the screw cap and the release was performed at 37°C. Aliquots of 500 μL organic solvent were collected at specific time points (0.5hr, 2hr, 4hr, 6hr, 24hr, 48hr, 72hr, 96hr, 8dys, 16dys, and 21dys) and replaced by the same amount of fresh solvent to maintain constant volume.

3 RESULTS AND DISCUSSION

3.1 Extraction Efficiency of Curcumin from PEG-PLGA nanoparticles

Table 2 shows efficient extraction of curcumin from PEG-PLGA nanoparticles with ethyl acetate after resuspension of the nanoparticles in phosphate buffer solution at different pH values. During the release of curcumin using 2mL of aqueous suspended PEG-PLGA curcumin nanoparticles and 4mL of ethyl acetate, 21.2 µg of curcumin are expected theoretically to be extracted. The theoretical amount of curcumin is calculated by multiplying the experimental encapsulation rate (0.530 µg curcumin/mg construct) with the total solid concentration in the suspension (20 mg/mL).

Table 2. Extraction efficiency of curcumin with ethyl acetate.

Sample	pH	Curcumin Extracted (µg)	STD ±	Theoretical Mass of Curcumin (µg)	Extraction Efficiency (%)
20 mg/mL PEG-PLGA curcumin nanoparticles in PBS	7.4	18.59	2.40	21.2	87.69
	5	16.98	2.62		80.10
	2	16.66	0.60		78.58

3.2 Degradation of Curcumin in Phosphate Buffer

The degradation of released curcumin from PEG-PLGA nanoparticles in phosphate buffer solution at pH 7.4, pH 5, and pH 2 is presented in **Figure 15**. The results confirm that curcumin

degrades at faster rate in pH 7.4. Around 70% of curcumin degrades after 24 hours of incubation at this pH. At pH 2 curcumin degradation is 50% in 24 hours. The fast degradation of curcumin at low pH may be attributed to the rapid degradation of PLGA at low pH. Therefore, curcumin is not well protected. PLGA degradation occurs by water uptake producing acidic oligomers. The acculumation of acid oligomers leads to an autocatalysis of PLGA and its degration.[30] Curcumin encapsulated in PEG-PLGA shows some stability in pH 5. After 24 hours, only 20% of curcumin degrades. At 96 hours about 45% of curcumin is degraded.

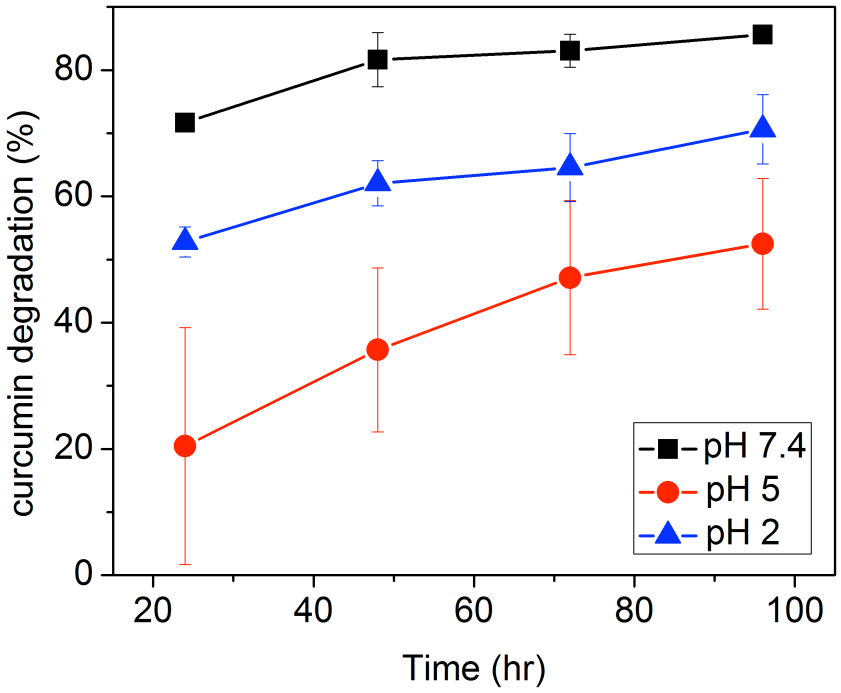

Figure 15. Curcumin degradation in phosphate buffer of three pH values at room temperature.

3.3 Physicochemical Properties of Curcumin Nanoparticles

The encapsulation efficiency of curcumin in PLGA and PEG-PLGA nanoparticles was determined by UV-vis spectrophotometer. High encapsulation efficiency more than 95% for both types of nanoformulations was achieved (**Table 3**).

Table 3. Encapsulation efficiency (EE) of curcumin in PLGA and PEG-PLGA polymeric nanoparticles.

Polymeric Nanoparticles	Experimental Measured Value (µg curcumin/mg construct)	Theoretical Value (µg curcumin/mg construct)	Encapsulation Efficiency (EE) %
PLGA curcumin	1.573	1.63	96.5 ± 4.52
PEG-PLGA curcumin	0.530	0.543	97.2 ± 4.88

PLGA curcumin nanoparticles suspended in 10mM phosphate buffer at pH 7.4 and pH 5 are about 100 nm in diameter. **Figure 16** shows the typical size distribution of these particles. However, the same PLGA curcumin nanoparticles suspended in phosphate buffer at pH 2 show a size in diameter of 288.5nm. Visible aggregates (**Figure 16**) are also found in this sample. This may be caused by protonation of PLGA at acidic environment since the stability of the particles is provided by charge repulsion. PEG-PLGA curcumin nanoparticles suspended in 10mM phosphate buffer show a similar size at various pH 182.7nm, 188.4nm, and 194.6nm, for pH 7.4, pH 5, and pH 2 respectively (**Figure 17**).

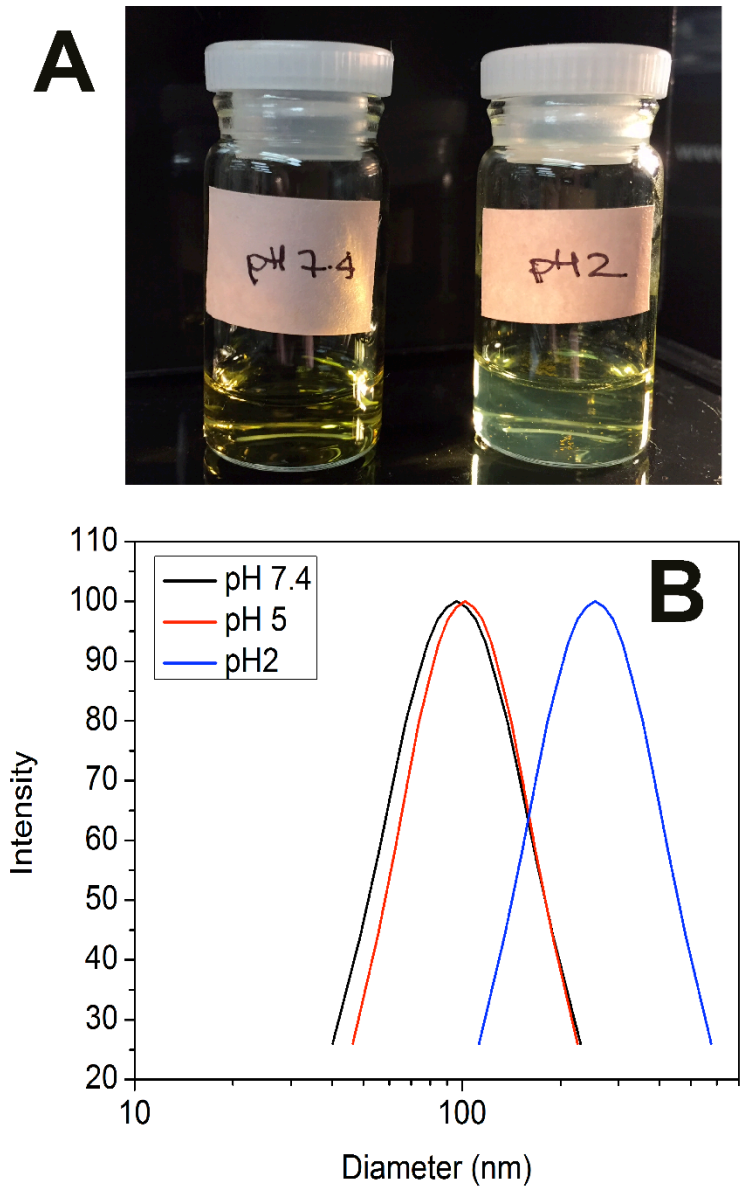

Figure 16. (A) PLGA curcumin nanoparticles in 10mM PBS pH 7.4 and pH 2. **(B)** Size distribution of PLGA curcumin nanoparticles.

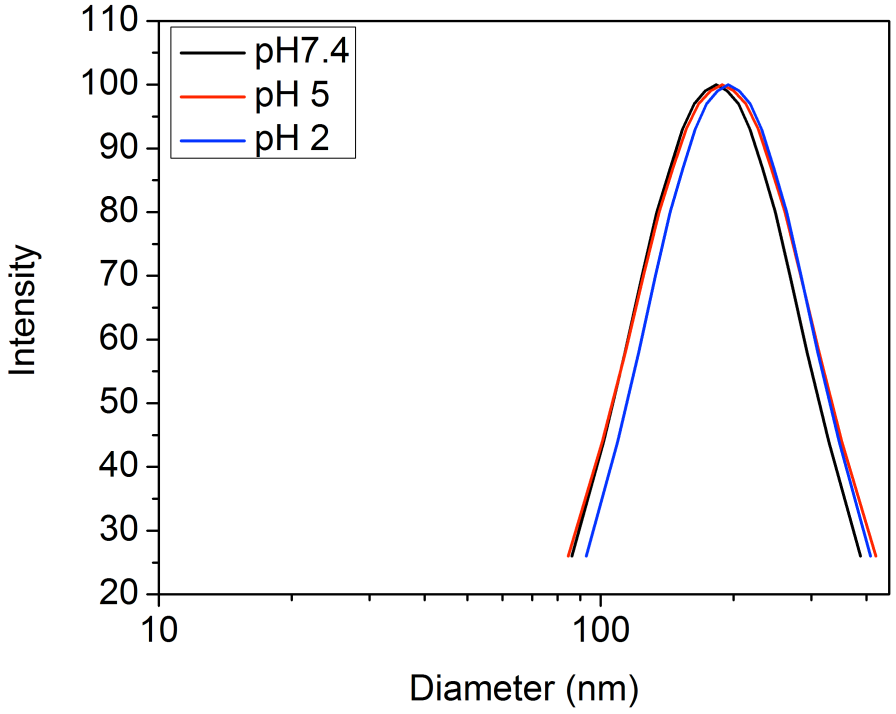

Figure 17. Size distribution of PEG-PLGA curcumin nanoparticles.

3.4 Measured Release of Curcumin from Nanoparticles Using Two-Phase *In Vitro* System

3.4.1 pH Dependence

The *in vitro* release of curcumin at 37°C from PLGA nanoparticles at both pH 5 and pH 7.4 show fast release of about 90% during the first 24 hours (**Figure 18**). The rapid drug release is mainly due to the contact of particles with the organic phase at the interface which may dissolve part of the particles for quick release of the drug. The difference of the release schedule at pH 5 and pH 7.4 is not obvious.

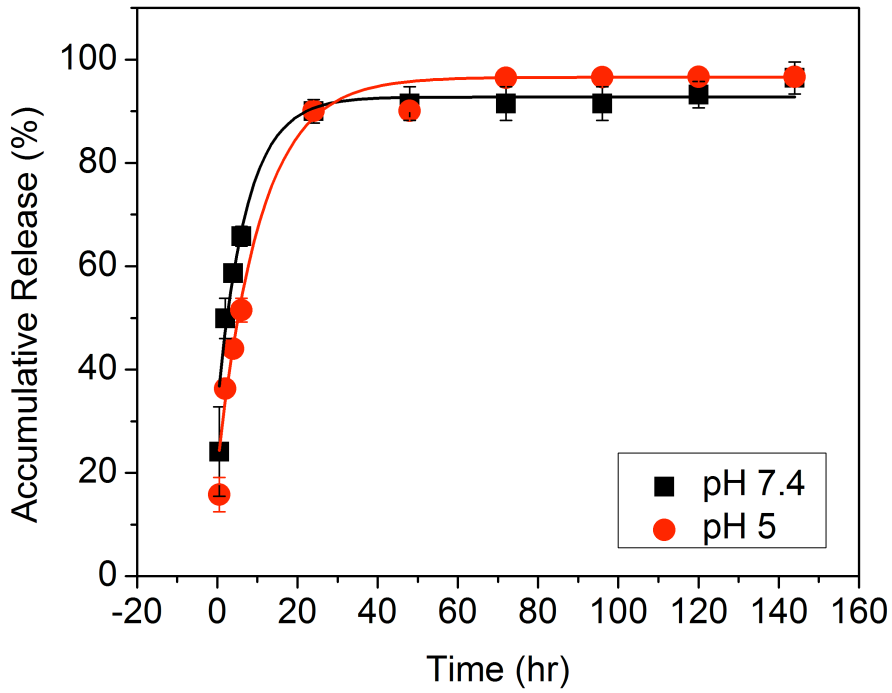

Figure 18. *In vitro* curcumin release from PLGA curcumin nanoparticles at different pH values.

The release of curcumin from PEG-PLGA nanoparticles at different pH values show similar profiles, which indicated that by this method the release of curcumin does not depend on the surface properties of the nanoparticles neither the degradation of the polymer. The release is mainly dominated by the fact that particles can randomly contact with the organic solvent at the liquid-liquid interface. This fast release of the drug from the polymeric nanoparticles is consistent with most *in vivo* studies. Although *in vivo* studies represent much more complicated mechanisms and dynamics, which cannot be represented by the simple two-phase system. One thing in common is that particles can be disassembled by either contact with the organic solvent or cell uptake. The traditional *in vitro* release systems such as dialysis which is completely diffusion-controlled does not represent particle disassembly and properties change.

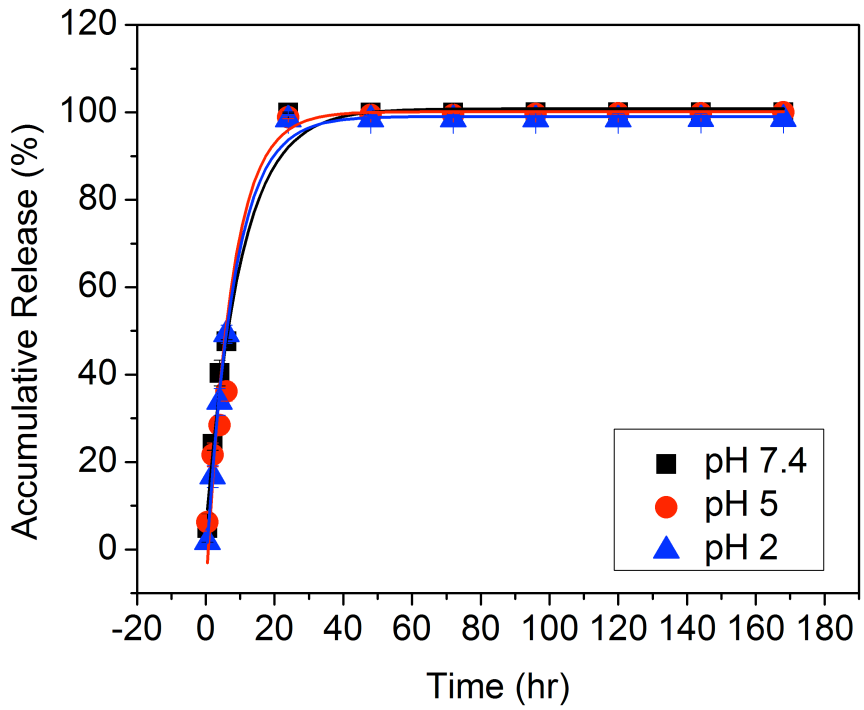

Figure 19. *In vitro* curcumin release from PEG-PLGA nanoparticles at different pH values.

3.4.2 Temperature Dependence

The *in vitro* release of curcumin from PEG-PLGA at pH 7.4 and different temperatures show different release profiles as expected. **Figure 20** shows that the release of curcumin at physiological temperature (37°C) is almost completed in 24 hours. At room temperature (22°C), the release of curcumin is much slower, which sustained for about 96 hours (**Figure 20**). This is mainly due to the less collision frequency of the nanoparticles with the organic-water interface.

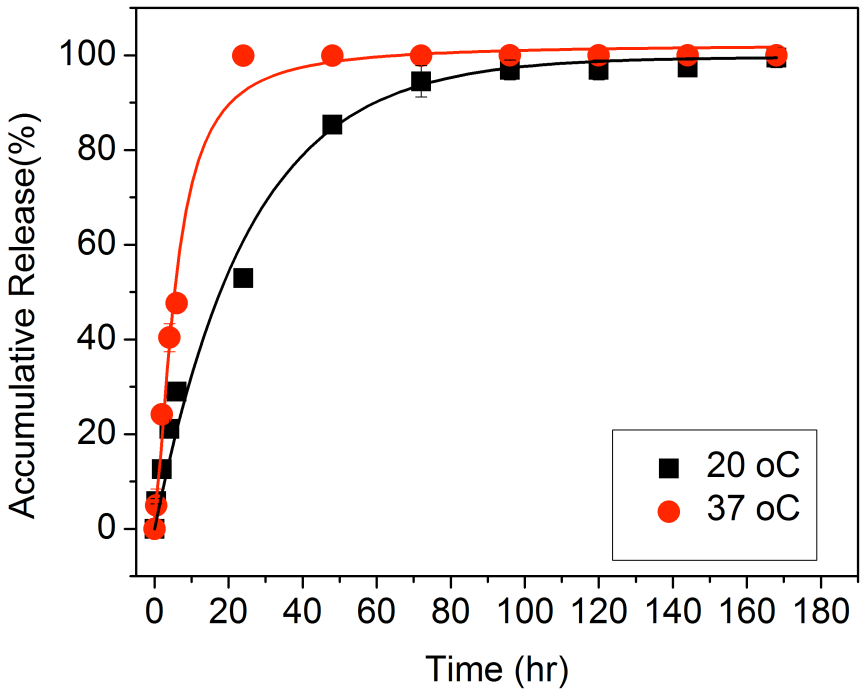

Figure 20. *In vitro* curcumin release from PEG-PLGA curcumin at different temperatures.

3.4.3 Volume Dependence

The *in vitro* release of curcumin using a two-phase system was also performed with different volume combinations between aqueous suspensions and the organic solvent. In this case, PEG-PLGA curcumin nanoparticles were resuspended in phosphate buffer at pH 7.4 at solid concentration of 20 mg/mL (11 µg/mL curcumin concentration) and the release of curcumin took place at 37°C.

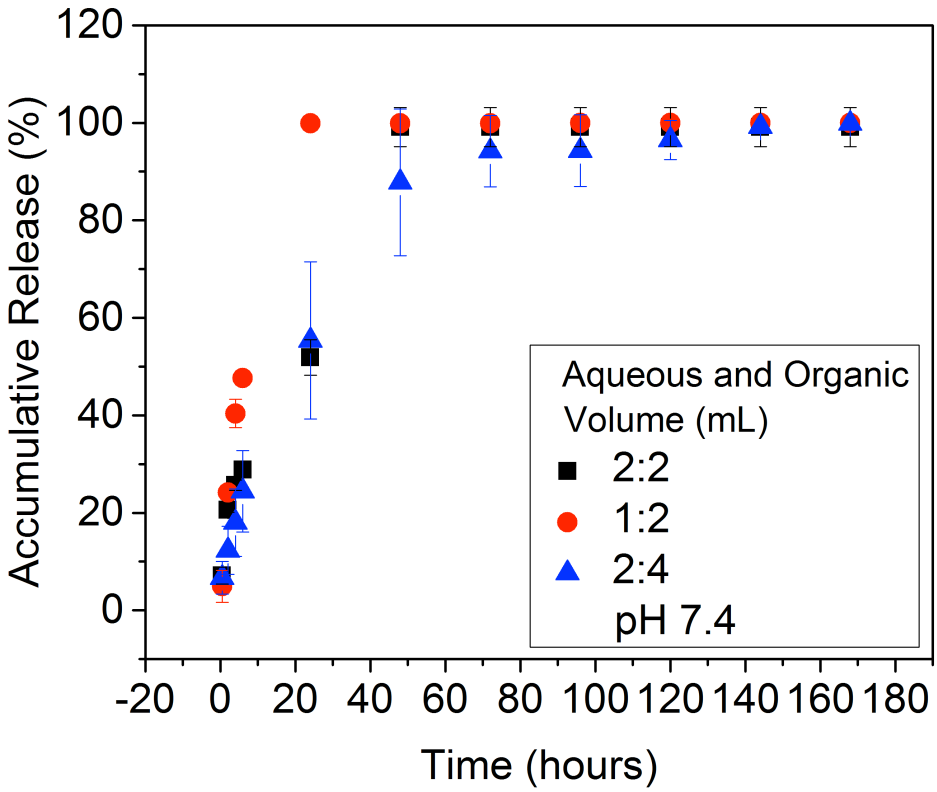

Figure 21. *In vitro* curcumin release from PEG-PLGA curcumin using different aqueous and organic volumes.

The results indicate that the release of curcumin is mainly influenced by the volume of the aqueous nanoparticles suspension. The release of curcumin is slower for larger aqueous nanoparticles suspension. The assumption is that with large volume of the aqueous suspension, the surface (of the interface) to the volume (of the suspension) ratio is reduced, and therefore the collision rate of the particles with the interface is relatively less. The amount of organic solvent show minor effect on curcumin release since the solubility of curcumin in the organic phase is very high and the organic phase presents a sink condition.

3.5 Measured Release of Curcumin from Nanoparticles using Two-Phase *In Vitro* Release System with Phospholipid Monolayers at the Liquid-Liquid Interface

3.5.1 L-α-PC

L-α-PC is a natural phospholipid extracted from chicken eggs. The *in vitro* release of curcumin from PLGA nanoparticles using L-α-PC at the liquid-liquid interface did not show a sustained release (**Figure 23**).

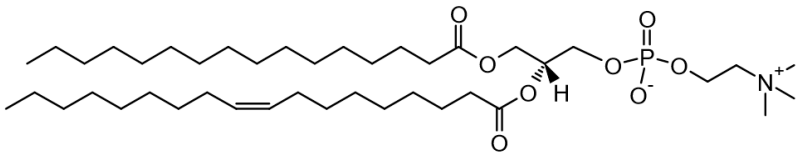

Figure 22. Molecular structure of predominant species of L-α-PC.

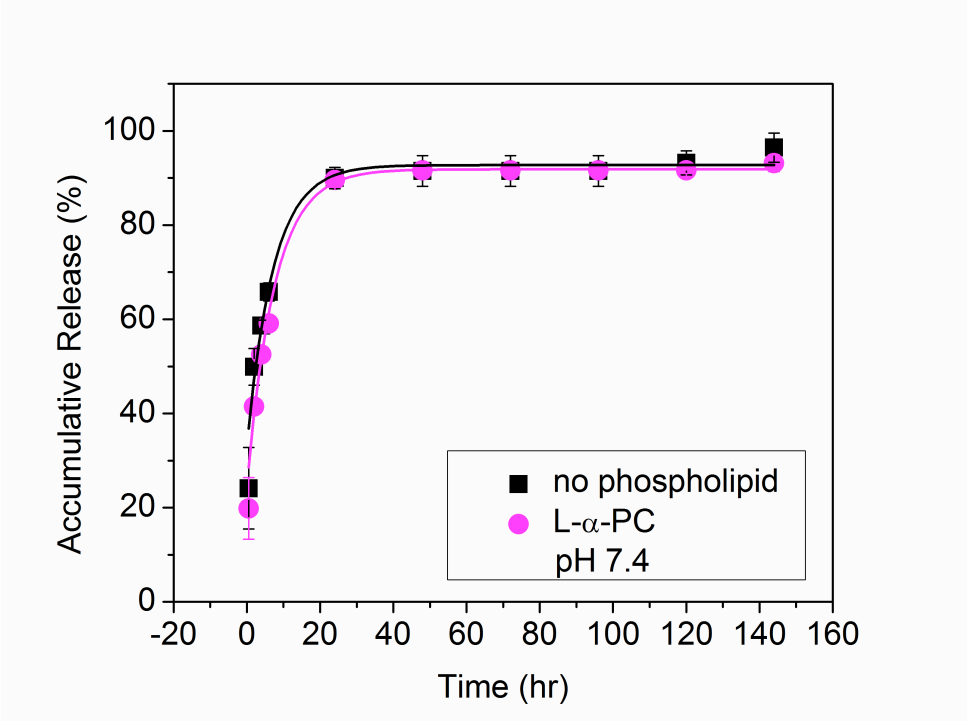

Figure 23. *In vitro* curcumin release with L-α-PC monolayer at the interface.

3.5.2 DPPC

The introduction of DPPC and DPPC-30% cholesterol monolayers at the liquid-liquid interface of the two-phase *in vitro* release model did not affect the release of curcumin from PEG-PLGA curcumin nanoparticles. The curves presented in **Figure 25** show the same release which is almost completed in 24 hours.

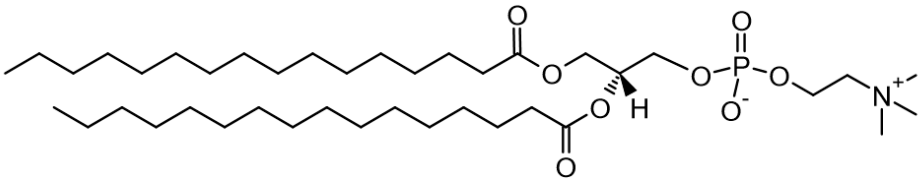

Figure 24. Molecular structure of DPPC.

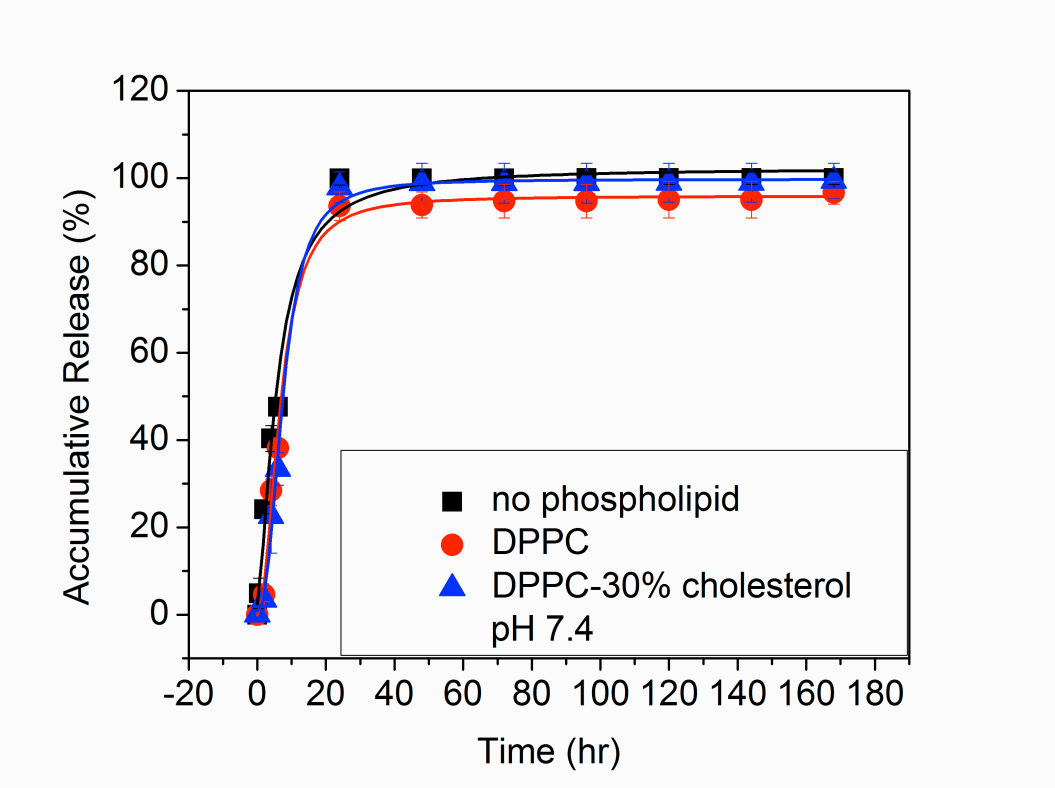

Figure 25. *In vitro* curcumin release with DPPC and DPPC-cholesterol monolayer at the liquid-liquid interface at 37°C compared to the release in the same system without any extra energy barrier at the interface.

The phase transition temperature of DPPC from gel to liquid is 41°C, which is close to body temperature. The release rate at a lower temperature was also measured. However, at 20°C, the *in vitro* release of curcumin using DPPC and DPPC-30% cholesterol monolayers at the liquid-liquid interface did not show any change either once compared to the release without phospholipids (**Figure 26**), although the release is slower at a lower temperature. This is consistent with the results described in the previous section.

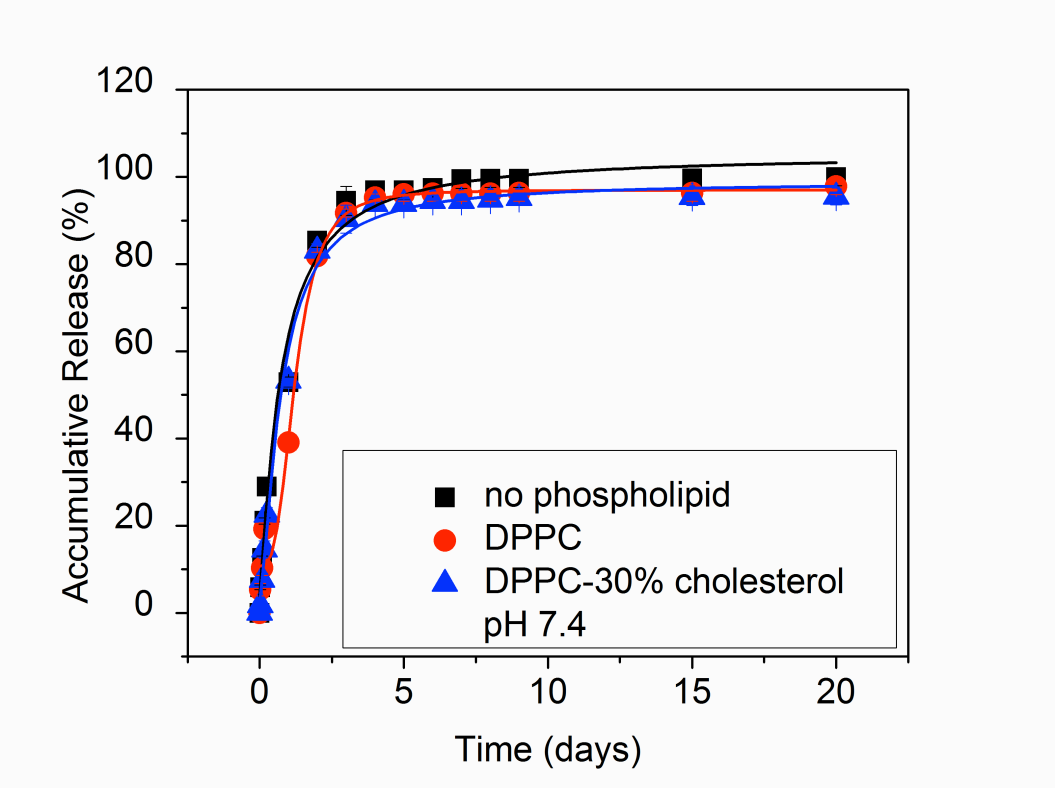

Figure 26. *In vitro* curcumin release with DPPC monolayer at 20°C.

3.5.3 DSPC

DSPC, another type of phospholipid, has a higher transition temperature of 55ºC. DSCP, DSPC-30% cholesterol, and DSPC-5%DPPE-PEG monolayers were used at the interface during the *in vitro* release measurements of curcumin from PEG-PLGA nanoparticles. **Figure 28** and **Figure 29** show the same rate for the release of curcumin using the above types of monolayers. The results indicated that these phospholipid monolayers regardless of their packing strengths did not provide a sufficient energy barrier to reduce the rate at which particles collide with the interface, and therefore the drug release was not sustained.

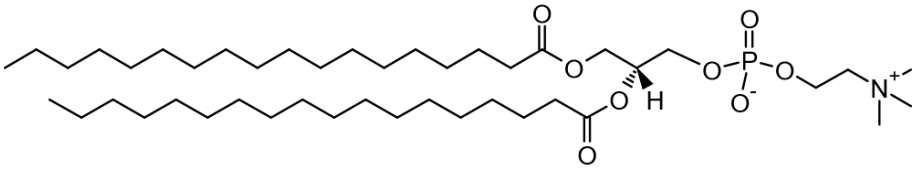

Figure 27. Molecular structure of DSPC.

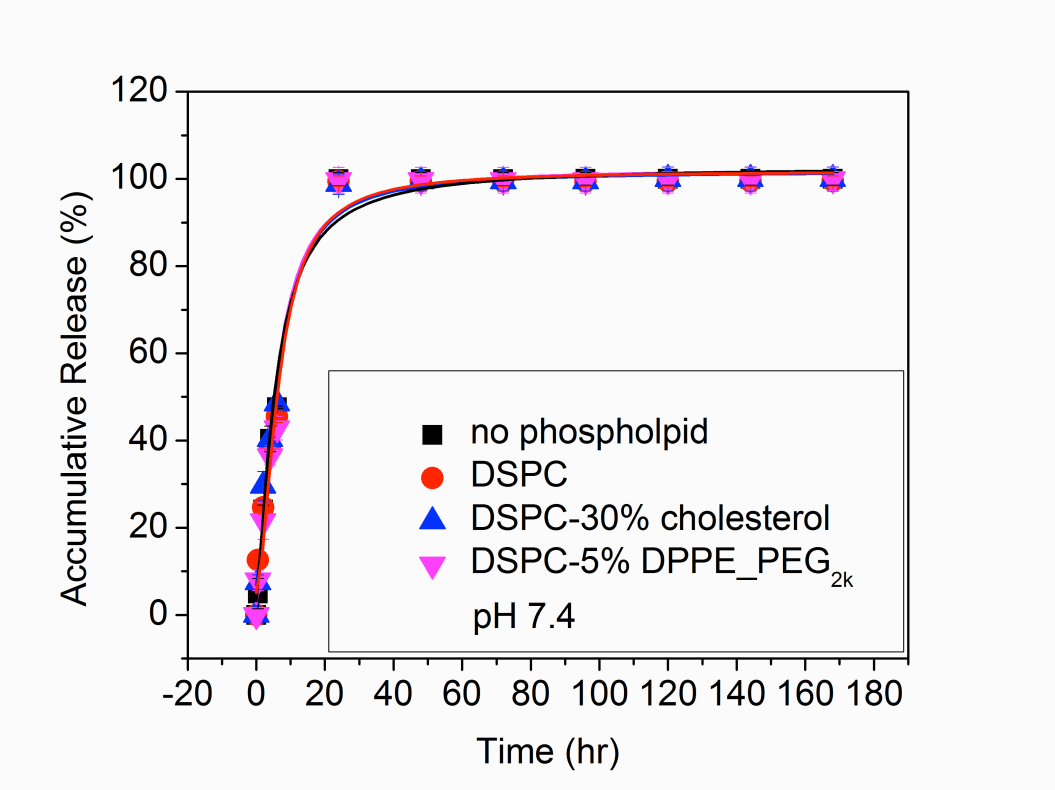

Figure 28. *In vitro* curcumin release with DSPC, DSPC-cholesterol, and DSPC-DPPE-PEG monolayers at the interface. The aqueous volume is 1mL and the organic phase volume is 2mL.

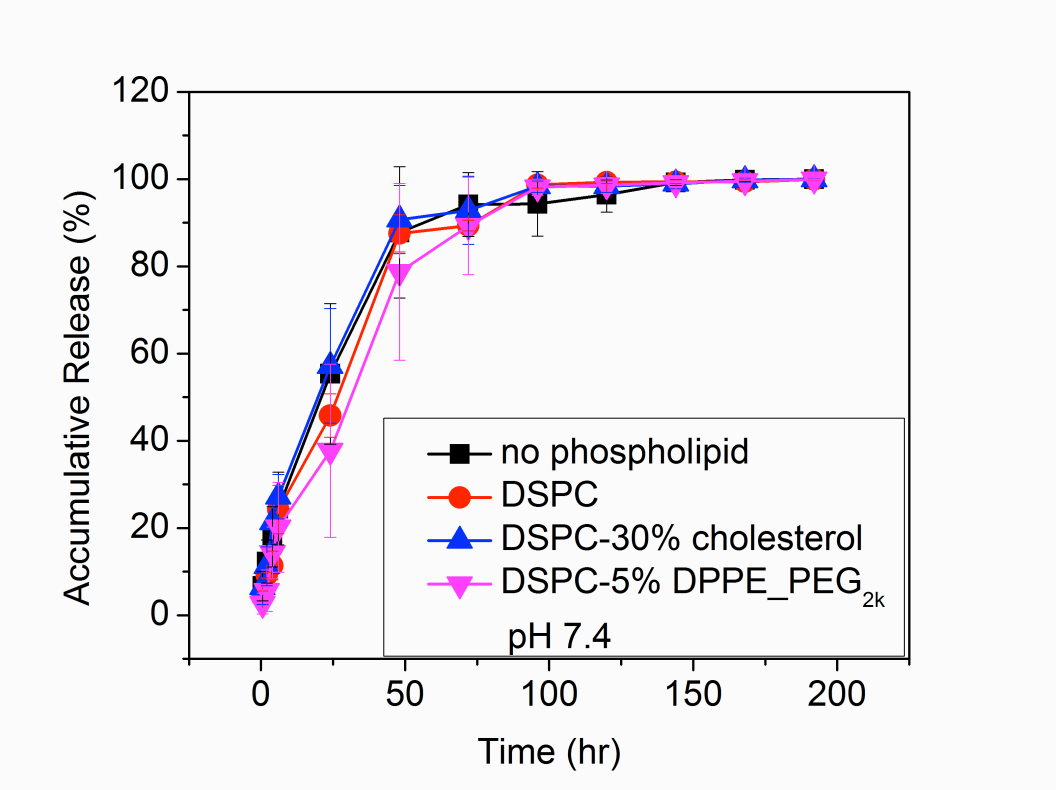

Figure 29. *In vitro* curcumin release with DSPC, DSPC-cholesterol, and DSPC-DPPE-PEG monolayers at the interface. The aqueous volume is 2mL and the organic phase volume is 4mL.

3.6 Measured Release of Curcumin from Nanoparticles Using Two-Phase *In Vitro* Release System with Dialysis Membrane at the Liquid-Liquid Interface

The *in vitro* release of curcumin from PEG-PLGA nanoparticles at both pH 5 and pH 7.4 using the glass cell and the dialysis membrane layer presented a sustained diffusion-controlled release. The percent release was calculated as mentioned above based on the final extraction value of curcumin rather than the initial extraction value to compensate the degradation of curcumin. The sustained release of curcumin at pH 7.4 was about 90% during the first 10 days. In contrast, the release of curcumin at pH 5 was sustained during 20 days with about 90% release.

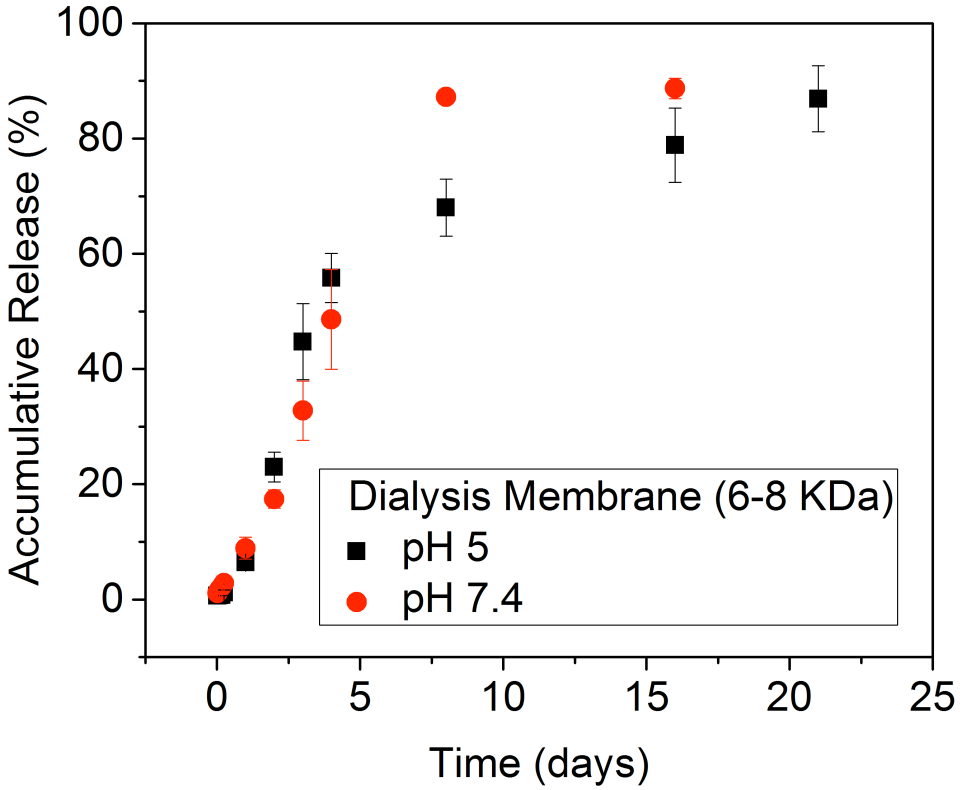

Figure 30. *In vitro* curcumin release in a glass cell with dialysis membrane at the interface.

3.7 Theoretical Analysis of Curcumin Release from Polymeric Nanoparticles to the Organic Phase Using a Pure Diffusion Model

3.7.1 Assumptions

The following assumptions were used for the theoretical analysis of curcumin diffusion to the organic phase from the nanoparticles.

The suspension of polymeric nanoparticles in the aqueous phase is homogeneous.

At the interface, the drug concentration is calculated by multiplying the partition coefficient, K, with the drug aqueous solubility.

The free drug in the aqueous solution is saturated.

The membrane pore size is big enough for the drug molecule to cross freely without any energy barrier, but small enough to prevent nanoparticles to go through. Therefore, there is concentration gradient near the membrane.

3.7.2 Important Parameters

The parameters were taken from the literature and listed in Table 4.

Table 4. Parameters used in the calculation.

Parameter	Value/Units
Partition coefficient of curcumin in water and in octanol[31]	log 3.68 or 4786
Diffusion coefficient in octanol[32]	0.00001 cm^2/s
Solubility of curcumin in water[33]	0.0004 mg/mL

3.7.3 One-dimensional Diffusion Model and Analytical Solution

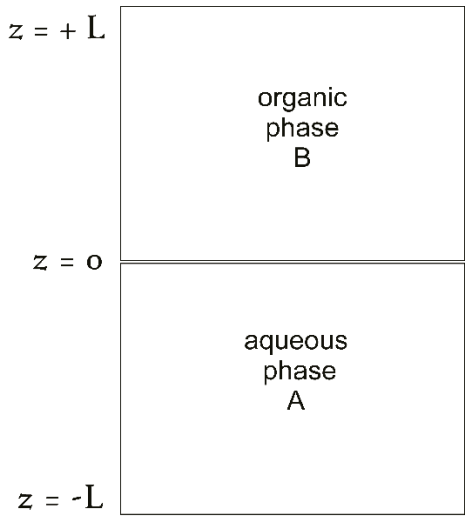

Figure 31. Schematic of two-phase system release model for analytical diffusion analysis.

The 1D dimensional diffusion model, boundary conditions, and initial condition are:

$$\frac{\partial C_B}{\partial t} = \mathcal{D}_B \nabla^2 C_B \qquad (5)$$

$$I.C. \quad at \quad t = 0\,, \quad C_B = 0$$

$$B.C.1 \quad at \quad z = 0, \quad C_B = KC_A$$

$$B.C.2 \quad at \quad z = L, \quad \frac{\partial C_B}{\partial z} = 0$$

The equation and boundary and initial conditions are non-dimensionalized by the following:

$$\Gamma = \frac{C_B}{KC_A} \qquad \xi = \frac{z}{L} \qquad \tau = \frac{t}{t_\propto} = \frac{\mathcal{D}_B t}{L^2}$$

The non-dimensionalized equation and boundary and initial conditions are:

$$\frac{\partial \Gamma}{\partial \tau} = \frac{\partial^2 \Gamma}{\partial \xi^2} \qquad (6)$$

$$I.C. \qquad at \qquad \tau = 0, \quad \Gamma = 0$$

$$B.C.1 \quad at \qquad \xi = 0, \quad \Gamma = 1$$

$$B.C.2 \quad at \qquad \xi = 1, \quad \frac{\partial \Gamma}{\partial \xi} = 0$$

The preceding partial differential equations were analytically solved by the method of separation of variables. The details are presented in Appendix A. The analytical solution of the curcumin concentration as a function of time and distance from the interface was plotted using MATLAB (**Figure 32**). The dimensions were restored using the parameters listed in **Table 4**.

$$C_B(t,z) = C_A K - \sum_{n=0}^{\infty} \frac{4C_A K}{(2n+1)\pi} \sin\left[\left(\frac{2n+1}{2L}\right)\pi z\right] e^{-\left[\left(\frac{2n+1}{2L}\right)\pi\right]^2 tD} \qquad (7)$$

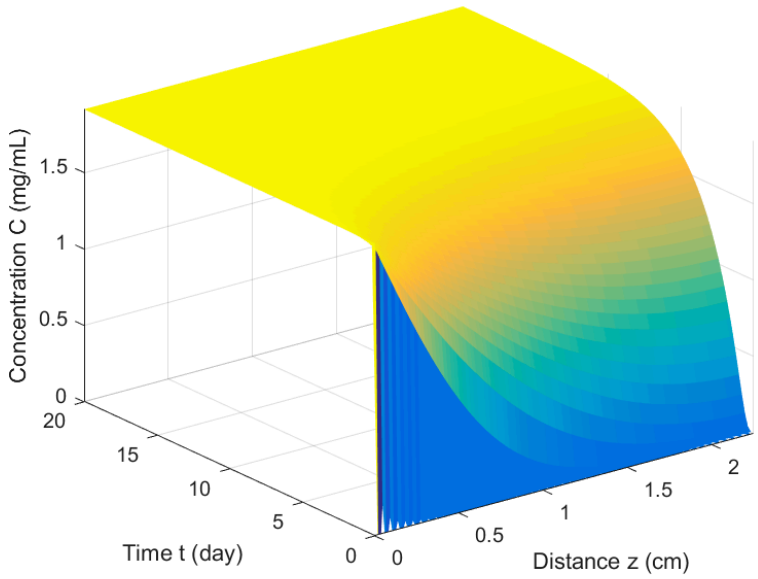

Figure 32. Curcumin concentration in the organic phase as a function of time and distance from the interface.

Figure 33 represents the percentage of released curcumin as a function of time at the top surface (z = L) of the organic solvent. The profile shows a sustained released of curcumin of about 90% during 10 days.

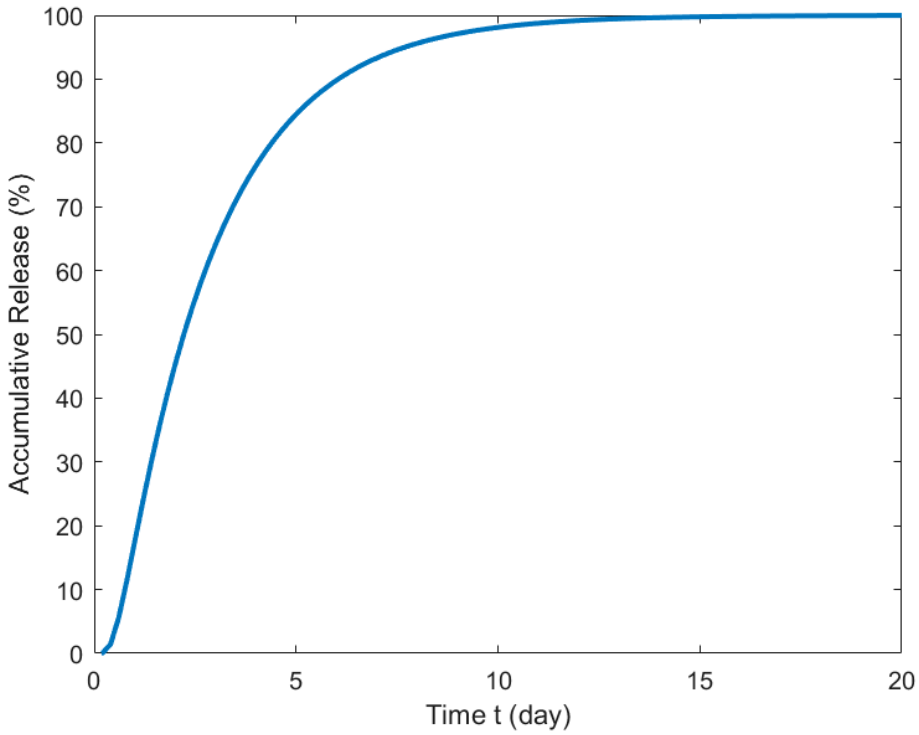

Figure 33. Curcumin released at organic phase position z = L.

Figure 34 shows how the amount of released curcumin changes with distance in the organic phase at different time points. At time t=0, no curcumin is present in the organic phase. At time t=10 days, almost 100% of curcumin is released to the organic phase.

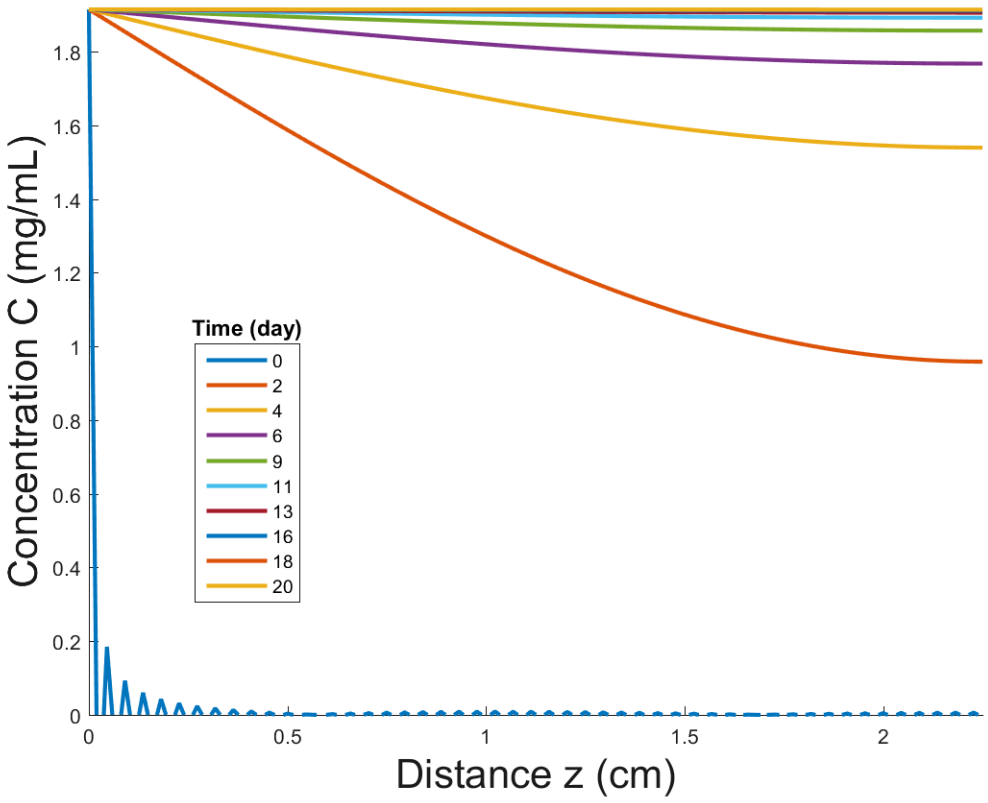

Figure 34. Curcumin release as function of distance for various times.

The mathematical analysis was also performed with different diffusivities and different partition coefficients to test the sensitivity of those two parameters in the release of curcumin. Partition coefficients did not affect the release profile while diffusivity was kept constant (**Figure 35**). However, by changing the diffusivity, the release profile was significantly varied, since this is a diffusion-controlled process. **Figure 36** shows the change in the release profile using a range of diffusivities and a constant partition coefficient of 4786. The release of curcumin was faster as diffusivity increased. All graphical solutions for this mathematical method were performed using the parameters set out in **Table 4**. Theses parameters do not correspond to the experimental conditions used in the present study. In future, at least the diffusivity of the system needs to be measured.

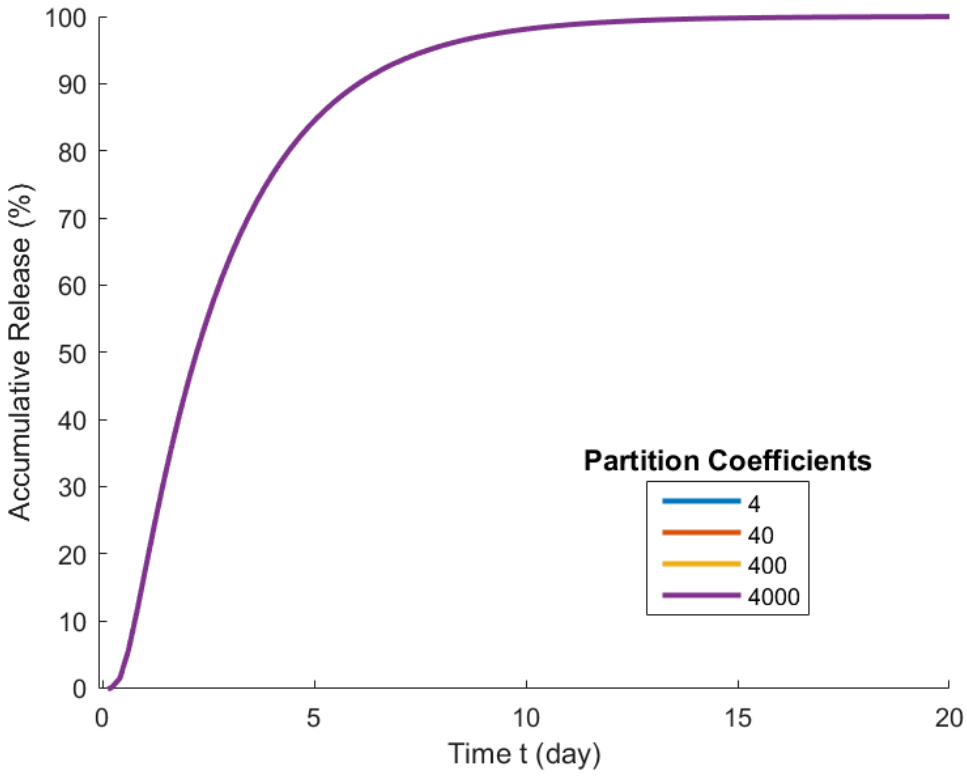

Figure 35. Concentration-time profiles of curcumin diffusion at various partition coefficients.

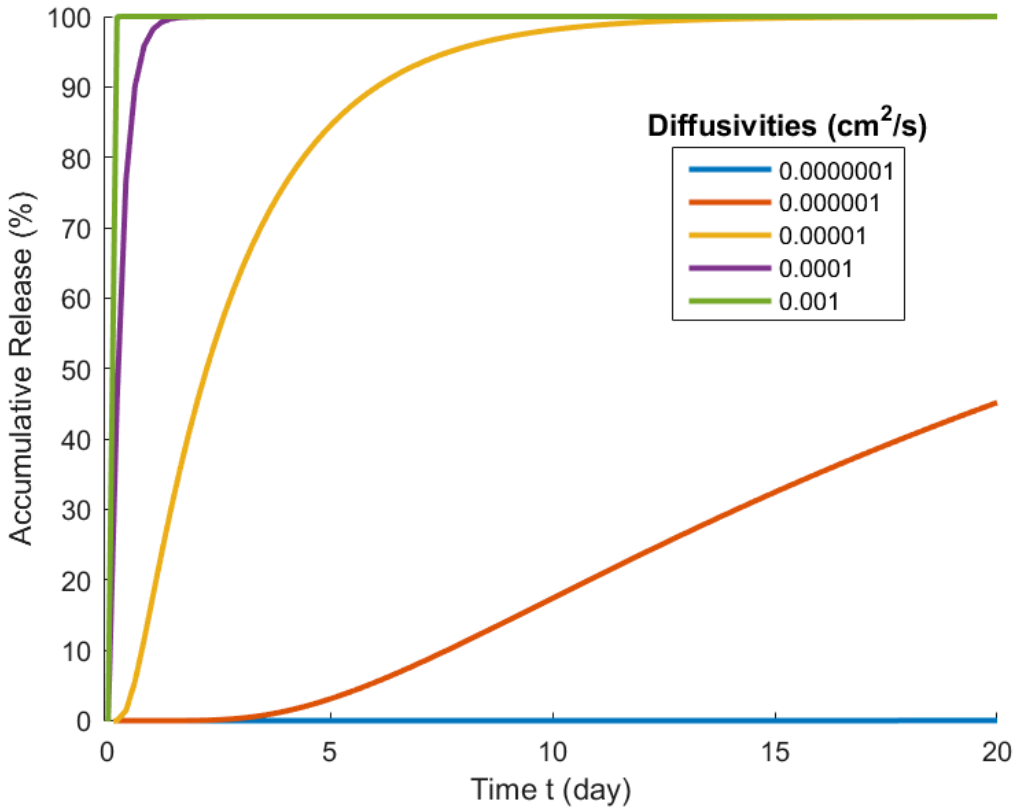

Figure 36. Concentration-time profiles of curcumin diffusion at different diffusivities.

4 CONCLUSIONS

Efficient, easy, and low-cost *in vitro* release methods using a two-phase system were developed for the study of the release of hydrophobic compounds from polymeric nanoparticles. The first *in vitro* release model with no biological barrier representation at the liquid-liquid interface showed a rapid release of curcumin mainly dominated by the contact of particles with the organic solvent at the interface. In this case, the *in vitro* release was independent of polymer degradation and pH. The addition of phospholipid and membrane protein molecules as monolayers with different packing strengths at the liquid-liquid interface of the two-phase system did not provide sustained release of curcumin. The introduction of a dialysis membrane layer at the interface of the two liquids completely prevented the contact of particles with the interface and provided a sustained diffusion-controlled release of curcumin. A simple one-dimensional diffusion model was used to briefly analyze the release of curcumin from the nanoparticles to the organic solvent. The theoretical analysis showed the sensitivity of diffusivity and partition coefficient in the release profile of curcumin.

APPENDIX A

ANALYTICAL SOLUTION OF THE PDE POF 1D DIFFUSION MODEL

Complete analytical solution to the diffusion partial differential equations presented in Section 3.7.3 by the separation of variables method.

Continuity Equation

$$c\left(\frac{\partial X_B}{\partial t} + \left(v \cdot \underline{\nabla} X_B\right)\right) = -\left(\underline{\nabla} \cdot \underline{J}_B\right) + r_B \qquad (1)$$

Assuming there is no convection for stationary liquids and no chemical reaction

$$\underline{v} = 0 \text{ and } r_B = 0$$

and substituting Fick's Law

$$\underline{J}_B = -c\mathcal{D}_B \underline{\nabla} X_B \text{ where } X_B = \frac{C_B}{c}$$

Then,

$$c\frac{\partial}{\partial t}\left(\frac{C_B}{c}\right) = c\mathcal{D}_B \nabla^2 \frac{C_B}{c} \qquad (2)$$

Simplifying, the Diffusion Equation or Fick's 2nd Law of Diffusion is obtained

$$\frac{\partial C_B}{\partial t} = \mathcal{D}_B \nabla^2 C_B \qquad (3)$$

$$I.C.\ \ at\ \ \ t = 0\,,\ \ C_B = 0$$

$$B.C.1\ \ at\ \ \ z = 0,\ \ C_B = KC_A$$

$$B.C.2\ \ at\ \ \ z = L,\ \ \frac{\partial C_B}{\partial z} = 0$$

Introducing dimensionless variables

$$\Gamma = \frac{C_B}{KC_A} \qquad \xi = \frac{z}{L} \qquad \tau = \frac{t}{t_\propto} = \frac{\mathcal{D}_B t}{L^2}$$

$$\frac{\partial \Gamma}{\partial \tau} = \frac{\partial^2 \Gamma}{\partial \xi^2} \qquad (4)$$

$$I.C. \qquad at \qquad \tau = 0, \quad \Gamma = 0$$

$$B.C.1 \quad at \qquad \xi = 0, \quad \Gamma = 1$$

$$B.C.2 \quad at \qquad \xi = 1, \quad \frac{\partial \Gamma}{\partial \xi} = 0$$

Solving the PDE (4) by the separation of variables method

$$\Gamma(\xi, \tau) = \Gamma_H(\xi, \tau) + \Gamma_P(\xi) \qquad (5)$$

Particular Inhomogeneous Solution: Steady State

$$(t \to \infty) \quad \frac{\partial \Gamma}{\partial \tau} = 0$$

$$\frac{\partial^2 \Gamma_P}{\partial \xi^2} = 0 \qquad (6)$$

$$\Gamma_P = C_1 \xi + C_2 \qquad (7)$$

Applying B.C. 1

$$B.C.1 \quad at \quad \xi = 0, \quad \Gamma = 1$$

$$1 = 0 + C_2$$

$$C_2 = 1$$

Applying B.C. 2

$$B.C.2 \quad at \quad \xi = 1, \quad \frac{\partial \Gamma}{\partial \xi} = 0$$

$$\frac{\partial \Gamma_P}{\partial \xi} = C_1$$

$$C_1 = 0$$

The particular solution is

$$\Gamma_P = 1 \qquad (8)$$

Homogeneous Solution:

$$\frac{\partial \Gamma_H}{\partial \tau} = \frac{\partial^2 \Gamma_H}{\partial \xi^2} \quad (9)$$

$$IC. \quad at \quad \tau = 0, \quad \Gamma = 0$$

$$B.C.1 \quad at \quad \xi = 0, \quad \Gamma = 0$$

$$B.C.2 \quad at \quad \xi = 1, \quad \frac{\partial \Gamma}{\partial \xi} = 0$$

$$\Gamma(\tau, \xi) = G(\tau)\, F(\xi) \quad (10)$$

Taking the partial derivatives of Γ with respect to τ and ξ

$$\frac{\partial \Gamma_H}{\partial \tau} = F\, \frac{dG}{d\tau}$$

$$\frac{\partial^2 \Gamma_H}{\partial \xi^2} = G\, \frac{d^2 F}{d\xi^2}$$

Substituting the partial derivatives into equation (9)

$$F\, \frac{dG}{d\tau} = G\, \frac{d^2 F}{d\xi^2} \quad (11)$$

$$\frac{1}{G}\frac{dG}{d\tau} = \frac{1}{F}\frac{d^2 F}{d\xi^2} = -C^2$$

Separating the variables

$$\frac{dG}{d\tau} = -C^2 G$$

$$\int \frac{dG}{G} = -C^2 \int d\tau + lnA$$

$$\ln G = -C^2\tau + \ln A$$

$$G = Ae^{-C^2\tau}$$

$$\frac{d^2F}{d\xi^2} + C^2F = 0$$

$$F = B\ sin(c\xi) + Ccos(c\xi)$$

Applying B.C. 1

$$B.C.1 \quad at \quad \xi = 0, \quad F = 0$$

$$0 = B\sin(0) + C\cos(0)$$

$$C = 0$$

Applying B.C. 2

$$B.C.2 \quad at \quad \xi = 1, \quad \frac{\partial F}{\partial \xi} = 0$$

$$\frac{\partial F}{\partial \xi} = B\ ccos(c\xi) - C\ csin(c\xi)$$

$$0 = B\ ccos(c)$$

$$c = \left(n + \frac{1}{2}\right)\pi, \qquad n = 0,1,2\ldots.$$

$$F = B\ \sin(c\xi)$$

Substituting G and F into equation (10)

$$\Gamma_H(\tau, \xi) = A\ e^{-C^2\tau} B sin(c\xi) \qquad (12)$$

$$\Gamma_H(\tau, \xi) = \sum_{n=0}^{\infty} D_n \sin(c\xi)\, e^{-c^2\tau} \qquad (13)$$

Combining the particular and homogeneous solutions into equation (5) then,

$$\Gamma(\tau, \xi) = 1 + \sum_{n=0}^{\infty} D_n \sin\left[\left(n + \frac{1}{2}\right)\pi\xi\right] e^{-c^2\tau} \qquad (14)$$

Applying the I.C. and using the orthogonality relation, D_n is obtained

$$I.C. \quad at \quad \tau = 0, \quad \Gamma = 0$$

$$\int_0^1 \sin\left[\left(m + \tfrac{1}{2}\right)\pi\xi\right] d\xi \left\| -1 = \sum_{n=0}^{\infty} D_n \sin\left[\left(n + \tfrac{1}{2}\right)\pi\xi\right] \right\|$$

$$-\int_0^1 sin\left[\left(m+\tfrac{1}{2}\right)\pi\xi\right]d\xi = \sum_{n=0}^{\infty} D_n \int_0^1 \sin\left[\left(n+\frac{1}{2}\right)\pi\xi\right] sin\left[\left(m+\tfrac{1}{2}\right)\pi\xi\right]d\xi \qquad (15)$$

Solving the integral

$$\int \sin(ax)\,dx = -\frac{1}{a}\cos(ax)$$

$$\int sin^2(ax)\,dx = \frac{x}{2} - \frac{\sin 2(ax)}{4a}$$

$$\frac{1}{\left(n+\frac{1}{2}\right)\pi}\left[cos\left(n+\tfrac{1}{2}\right)\pi\xi\right]_0^1 = D_n\left[\frac{\xi}{2} - \frac{sin2\left(n+\frac{1}{2}\right)\pi\xi}{4\left(n+\frac{1}{2}\right)\pi}\right]_0^1$$

$$-\frac{1}{\left(n+\frac{1}{2}\right)\pi} = D_n\left[\frac{\frac{1}{2}\left(n+\frac{1}{2}\right)\pi\xi - \frac{1}{4}sin2\left(n+\frac{1}{2}\right)\pi\xi}{\left(n+\frac{1}{2}\right)\pi}\right]_0^1$$

$$-1 = D_n\left[\frac{1}{2}\left(n+\tfrac{1}{2}\right)\pi\right]$$

$$D_n = -\frac{2}{\left(n+\frac{1}{2}\right)\pi} \qquad (16)$$

Solution:

$$\Gamma(\tau,\xi) = \Gamma_P + \Gamma_H$$

$$\Gamma(\tau,\xi) = 1 - \sum_{n=0}^{\infty} D_n \sin(c\xi) e^{-c^2\tau}$$

Substituting D_n

$$\Gamma(\tau,\xi) = 1 - \sum_{n=0}^{\infty} \frac{4}{(2n+1)\pi} \sin\left[\left(n+\frac{1}{2}\right)\pi\xi\right] e^{-\left[\left(n+\frac{1}{2}\right)\right]^2 \tau} \qquad (17)$$

$$\frac{C_B(t,z)}{C_A K} = 1 - \sum_{n=0}^{\infty} \frac{4C_A K}{(2n+1)\pi} \sin\left[\left(\frac{2n+1}{2}\right)\pi\frac{z}{L}\right] e^{-\left[\left(\frac{2n+1}{2}\right)\pi\right]^2 \frac{tD}{L^2}}$$

$$C_B(t,z) = C_A K - \sum_{n=0}^{\infty} \frac{4C_A K}{(2n+1)\pi} \sin\left[\left(\frac{2n+1}{2L}\right)\pi z\right] e^{-\left[\left(\frac{2n+1}{2L}\right)\pi\right]^2 tD} \qquad (18)$$

APPENDIX B

MATLAB SCRIPTS

MATLAB script to plot the analytical concentration profile of curcumin in the organic solvent.

```
% Analytical Solution to Diffusion Analysis

% Important parameters
K = 4786;               % partition coefficient of curcumin in water/octanol
Ca = 0.0004;            % solubility of curcumin in water (mg/mL)
D = 0.00001;              % diffusivity of curucmin (cm^2/day)
L = 2.25;               % height of organic phase (cm)

% Boundary condition at z=0
Cb = K*Ca;


x = linspace (0, 2.25, 100);
t = linspace (0, 20, 100);



for m = 1:1:length(t)
    for i = 1:1:length(x)
    summation = 0;
    for n = 0:1:100             % solves the summation from 0 to 100 terms
        Dn = (4*Cb)/((2*n+1)*pi);
        summation = summation+ Dn * exp(-D*3600*24*t(m)*(((2*n+1)*pi)/(2*L))^2)...
                    * sin((((2*n+1)*pi)/(2*L))*x(i));
    end
    c(m,i) = Cb - summation;    % calculates the concentration profile
    end
end

cp = (c/Cb)*100;

% Plotting the solution
figure (1)
surf(x,t,c,'edgecolor','none')
xlabel ('Distance z (cm)', 'fontsize',20,'fontname','arial');
ylabel ('Time t (s)','fontsize',20,'fontname','arial');
zlabel ('Concentration C (mg/mL)','fontsize',20,'fontname','arial');
axis ([0 L 0 20 0 Cb])

figure (2)
plot (t,cp(:,end),'LineWidth',2)
xlabel ('Time t (s)','fontsize',20,'fontname','arial');
ylabel ('Accumulative Release (%)','fontsize',20,'fontname','arial');
axis ([0 20 0 100])

figure (3)
hold all
for p = linspace(1,length(t),10)
    plot (x, c(p,:), 'LineWidth',2)
end

xlabel ('Distance z (cm)', 'fontsize',20,'fontname','arial');
ylabel ('Concentration C (mg/mL)','fontsize',20,'fontname','arial');
axis ([0 L 0 Cb])

hlegend = legend ('0','2','4','6','9','11','13','16','18','20');
hlegendaxes = axes ('Parent', hlegend.Parent, 'Units', hlegend.Units, 'Position', hlegend.Position,...
                    'Xtick',[],'YTick',[],'Color','none', 'YColor', 'none', 'XColor', 'none',.....
                    'HandleVisibility', 'off', 'HitTest', 'off');
htitle = title(hlegendaxes, 'Time (day)');
hlinks = linkprop([hlegend, hlegendaxes], {'Units', 'Position', 'Visible'});
setappdata(hlegendaxes, 'listeners', hlinks);
```

MATLAB script to plot the concentration profile of curcumin as a function of time for different diffusivities while keeping the partition coefficient of curcumin in the organic solvent constant.

```
% Analytical Solution to Diffusion Analysis

% Important parameters
K = 4786;              % partition coefficient of curcumin in water/octanol
Ca = 0.0004;           % solubility of curcumin in water (mg/mL)
L = 2.25;              % height of organic phase (cm)

% Boundary condition at z=0
Cb = K*Ca;

x = 2.25;
t = linspace (0, 20, 100);
d =[0.0000001 0.000001 0.00001 0.0001 0.001];

figure
xlabel ('Time t (day)','fontsize',20,'fontname','arial');
ylabel ('Accumulative Release (%)','fontsize',20,'fontname','arial');
axis ([-0.1 20 -0.1 100]);


for i=1:1:5
hold on

D = d(i)*3600*24;
    for m = 1:1:length(t)
            summation = 0;
        for n = 0:1:100                     % solves the summation from 0 to 100 terms
            Dn = (4*Cb)/((2*n+1)*pi);
            summation = summation + Dn * exp(-D*t(m)*(((2*n+1)*pi)/(2*L))^2)* sin(((2*n+1)*pi*x)/(2*L));
        end
        c(m) = ((Cb - summation)/Cb)*100;    % calculates the concentration profile
    end
plot (t,c,'LineWidth',2)

end


hlegend = legend ('0.0000001','0.000001','0.00001','0.0001','0.001');
hlegendaxes = axes ('Parent', hlegend.Parent, 'Units', hlegend.Units, 'Position', hlegend.Position,...
                    'Xtick',[],'YTick',[],'Color','none', 'YColor', 'none', 'XColor', 'none',......
                    'HandleVisibility', 'off', 'HitTest', 'off');
htitle = title(hlegendaxes, 'Diffusivities (cm^2/s)');
hlinks = linkprop([hlegend, hlegendaxes], {'Units', 'Position', 'Visible'});
setappdata(hlegendaxes, 'listeners', hlinks);
```

MATLAB script to plot the concentration profile of curcumin as a function of time for different partition coefficients while keeping the diffusivity of curcumin in the organic solvent constant.

```
% Analytical Solution to Diffusion Analysis

% Important parameters
d = 0.00001;           % diffusivity of curcumin in octanol (cm^2/s)
Ca = 0.0004;           % solubility of curcumin in water (mg/mL)
L = 2.25;              % height of organic phase (cm)

x = 2.25;
t = linspace (0, 20, 100);
K =[4 40 400 4000];

figure
xlabel ('Time t (day)','fontsize',20,'fontname','arial');
ylabel ('Accumulative Release (%)','fontsize',20,'fontname','arial');
axis ([-0.1 20 -0.1 100]);


for i=1:1:4
hold on

Cb = K(i)*Ca;
    for m = 1:1:length(t)
            summation = 0;
        for n = 0:1:100                    % solves the summation from 0 to 100 terms
            Dn = (4*Cb)/((2*n+1)*pi);
            summation = summation + Dn * exp(-d*3600*24*t(m)*(((2*n+1)*pi)/(2*L))^2)* sin(((2*n+1)*pi*x)/(2*L));
        end
        c(m) = ((Cb - summation)/Cb)*100;    % calculates the concentration profile
    end
plot (t,c,'LineWidth',2)

end


hlegend = legend ('4','40','400','4000');
hlegendaxes = axes ('Parent', hlegend.Parent, 'Units', hlegend.Units, 'Position', hlegend.Position,....
                    'Xtick',[],'YTick',[],'Color','none', 'YColor', 'none', 'XColor', 'none',....
                    'HandleVisibility', 'off', 'HitTest', 'off');
htitle = title(hlegendaxes, 'Partition Coefficients');
hlinks = linkprop([hlegend, hlegendaxes], {'Units', 'Position', 'Visible'});
setappdata(hlegendaxes, 'listeners', hlinks);
```

APPENDIX C

DESIGNS OF THE GLASS CELLS TO INCORPORATE DIALYSIS MEMBRANE

The final glass cell was achieved by several design and materials modifications. The initial design (A) was a stainless steel cell with precise dimensions; however, the main disadvantages of this design were cost and difficult sample collection. The next design (B) was a glass cell with no O-ring and rubber stopper at the sampling port. This design's disadvantages were evaporation, stopper compatibility issues with the organic solvent, and leakage. The third design was also a glass cell but with a Teflon O-ring and rubber stopper. The problem with this design was the solvent's evaporation mainly caused by the stopper material.

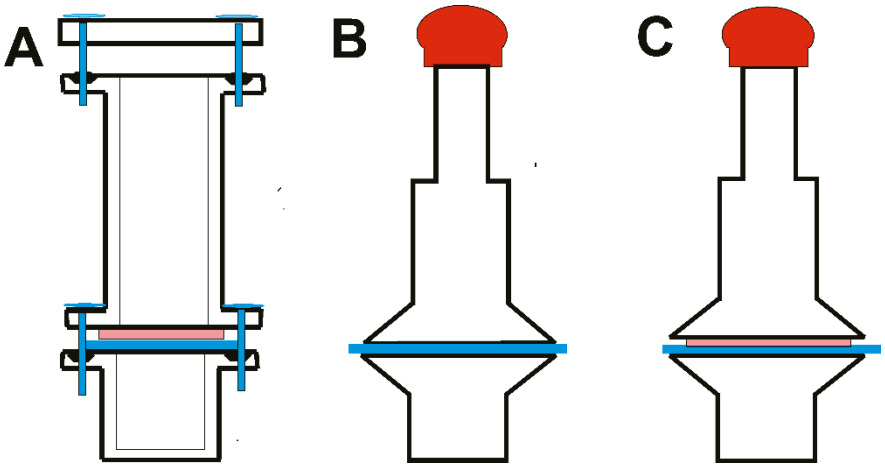

REFERENCES

1. Pinto Reis, C.; Neufeld, R. J.; Ribeiro, A. J.; Veiga, F. *Nanomedicine : nanotechnology, biology, and medicine* **2006,** 2, (1), 8-21.

2. M.L. Hans, A. M. L. *Current Opinion in Solid State asnd Materials Science* **2002,** 6, 319-327.

3. Shen, H.; Banerjee, A. A.; Mlynarska, P.; Hautman, M.; Hong, S.; Kapetanovic, I. M.; Lyubimov, A. V.; Liu, Y. *Journal of pharmaceutical sciences* **2012,** 101, (10), 3877-85.

4. Shen, H.; Hu, X.; Szymusiak, M.; Wang, Z. J.; Liu, Y. *Molecular pharmaceutics* **2013,** 10, (12), 4546-51.

5. Kumar, S. S.; Surianarayanan, M.; Vijayaraghavan, R.; Mandal, A. B.; MacFarlane, D. R. *European journal of pharmaceutical sciences : official journal of the European Federation for Pharmaceutical Sciences* **2014,** 51, 34-44.

6. Anand, P.; Nair, H. B.; Sung, B.; Kunnumakkara, A. B.; Yadav, V. R.; Tekmal, R. R.; Aggarwal, B. B. *Biochemical pharmacology* **2010,** 79, (3), 330-8.

7. He, C.; Hu, Y.; Yin, L.; Tang, C.; Yin, C. *Biomaterials* **2010,** 31, (13), 3657-66.

8. Mohanty, C.; Sahoo, S. K. *Biomaterials* **2010,** 31, (25), 6597-611.

9. Zou, P.; Helson, L.; Maitra, A.; Stern, S. T.; McNeil, S. E. *Molecular pharmaceutics* **2013,** 10, (5), 1977-87.

10. Shen, H.; Hong, S.; Prud'homme, R. K.; Liu, Y. *Journal of Nanoparticle Research* **2011,** 13, (9), 4109-4120.

11. Akbulut, M.; Ginart, P.; Gindy, M. E.; Theriault, C.; Chin, K. H.; Soboyejo, W.; Prud'homme, R. K. *Advanced Functional Materials* **2009,** 19, (5), 718-725.

12. Zhang, C.; Pansare, V. J.; Prud'homme, R. K.; Priestley, R. D. *Soft Matter* **2012,** 8, (1), 86-93.

13. Hu, X.; Huang, F.; Szymusiak, M.; Liu, Y.; Wang, Z. J. *The Journal of pharmacology and experimental therapeutics* **2015,** 352, (3), 420-8.

14. Mittal, G.; Sahana, D. K.; Bhardwaj, V.; Ravi Kumar, M. N. *Journal of controlled release : official journal of the Controlled Release Society* **2007,** 119, (1), 77-85.

15. Manisha P. Desai, V. L., Elke Walter, Robert J. Levy, and Gordon L. Amidon. *Pharmaceutical research* **1997,** 14, (11), 1568-1573.

16. T. Jung, W. K., A. Breitenbach, E. Kaiserling, J. X. Xiao, T. Kissel. *European Journal of Pharmaceutics and Biopharmaceutics* **2000**, 147-160.

17. Win, K. Y.; Feng, S. S. *Biomaterials* **2005,** 26, (15), 2713-22.

18. Pawel Wydro, a. K. H.-W. *J. Phys. Chem. B* **2007,** 111, 2495-2502.

19. Hac-Wydro, K.; Wydro, P. *Chemistry and physics of lipids* **2007,** 150, (1), 66-81.

20. Kwangmeyung Kim, C. K., and Youngro Byun *Langmuir : the ACS journal of surfaces and colloids* **2001,** 17, 5066-5070.

21. Kim, Y.-H.; Tero, R.; Takizawa, M.; Urisu, T. *Japanese Journal of Applied Physics* **2004,** 43, (6B), 3860-3864.

22. Tzung-Han Chou, I.-M. C. *Colloids and Surfaces B: Biointerfaces 27* **2003,** 27, 333-344.

23. Tzung-Han Chou, I.-M. C. *Colloids and Surfaces A: Physicochem. Eng. Aspects* **2002,** 211, 267-274.

24. Peter Liljeroth, A. M., Vincent J. Cunnane, Anna-Kaisa Kontturi, and Kyosti Kontturi. *Langmuir : the ACS journal of surfaces and colloids* **2000,** 16, 6667-6673.

25. Sathyanarayana N. Gummadi, S. H., Jane Walent, William E. Watkins, and Anant K. Menon, Reconstitution and Assay of Biogenic Membrane-Derived Phospholipid Flippase Activity in Proteoliposomes. In *Methods in Molecular Biology*, Inc., B. S. H. P., Ed. Totowa, NJ, Vol. 228.

26. Mansour, H.; Wang, D.-S.; Chen, C.-S.; Zografi, G. *Langmuir* **2001,** 17, (21), 6622-6632.

27. Kwangmeyung Kim, C. K., and Youngro Bryun. *Langmuir* **2001,** 17, 5066-5070.

28. Robert A. Walker, J. C. C., and Geraldine L. Richmond. *Langmuir : the ACS journal of surfaces and colloids* **1997,** 13, 3070-3073.

29. Moghaddam, B.; Ali, M. H.; Wilkhu, J.; Kirby, D. J.; Mohammed, A. R.; Zheng, Q.; Perrie, Y. *International journal of pharmaceutics* **2011,** 417, (1-2), 235-44.

30. Zolnik, B. S.; Burgess, D. J. *J Control Release* **2007,** 122, (3), 338-44.

31. Reiko Yutami, S.-y. M., Reiko Teraoka, and Shuji Kitagawa. *Chem. Pharm. Bull.* **2012,** 60, 989-994.

32. Boro, M. K. D. a. L. *World Journal of Pharmaceutical Research* **2014,** 3, (4), 2004-2028.

33. Yallapu, M. M.; Jaggi, M.; Chauhan, S. C. *Drug discovery today* **2012,** 17, (1-2), 71-80.

VITA

NAME:	Catalina Mogollon
EDUCATION:	B.S. Chemical Engineering, University of Illinois at Chicago, Chicago, Illinois, 2009
	M.S. Chemical Engineering, University of Illinois at Chicago, Chicago, Illinois, 2015
TEACHING:	Science and Health Department, St. Augustine College, Chicago, Illinois, Chemistry Adjunct Faculty, 2012
	Science and Health Department, St. Augustine College, Chicago, Illinois, Chemistry Tutor, 2009-2010
	Confederation of Latin American Students, CLAS, University of Illinois at Chicago, Tutor, 2008-2009
	Brain Hurricane Program at Carl Von Linne Elementary School, Chicago, Illinois, Math and Reading Tutor, 2008
EXPERIENCE:	DuPage Public Works Wastewater Treatment Plant (Messina Group), Woodridge, Illinois, Laboratory Technician, 2013
	EcoAlternativas S.A., Cumbaya, Ecuador, Laboratory Assistant, 2012
	UIC Chemical Engineering Department – Catalysis Lab, Chicago, Illinois, Undergraduate Research Assistant, 2008 - 2009

AWARDS:	Second Place Award, In the category of Environmental and Energy Conservation, Project titled Green Energy:Production of Alcohols From Switch Grass, 20th Anniversary EXPO 2009, UIC College of Engineering
	Certificate of Achievement, Latino Committee on University Affairs, University of Illinois at Chicago, 2009
PRESENTATIONS:	"Synthesis of Bimetallic Alloy Catalyst using Strong Electrostatic Adsorption," 19th Annual Argonne Symposium for Undergraduates in Science, Engineering and Mathematics, Argonne, Illinois, 2008